PERGAMON

Journal of Structural Geology 23 (2001) 1043–1065

JOURNAL OF STRUCTURAL GEOLOGY

www.elsevier.nl/locate/jstrugeo

# Deformation partitioning during transpression in response to Early Devonian oblique convergence, northern Appalachian orogen, USA

Gary S. Solar*, Michael Brown

*Laboratory for Crustal Petrology, Department of Geology, University of Maryland, College Park, MD 20742, USA*

Received 22 January 1999; accepted 23 August 2000

**Abstract**

Transpressive deformation was distributed heterogeneously within the Central Maine belt shear zone system, which formed in response to Early Devonian oblique convergence during the Acadian orogeny in the northern Appalachians. 'Straight' belts are characterized by tight folds, S > L fabrics and sub-parallel form lines, and asymmetric structures that together indicate dextral–SE-side-up kinematics. In contrast, intervening zones between 'straight' belts are characterized by open folds and L ≫ S fabrics. Within both types of zone, metasedimentary rocks have fabrics defined by the same minerals at the same metamorphic grade, including a penetrative, moderately to steeply NE-plunging mineral lineation. Thus, we interpret accumulation of plastic deformation and regional metamorphic (re-) crystallization to have been synchronous across the Central Maine belt shear zone system. Discordance between inclusion trails in regionally developed porphyroblasts of garnet and staurolite and matrix fabrics in 'straight' belt rocks records shortening by tightening of folds and greater reorientation of matrix fabrics with respect to porphyroblasts. Kinematic partitioning of flow was responsible for the contrasting states of finite deformation recorded in the Central Maine belt shear zone system. Perturbations in the flow were caused by serially developed thrust-ramp anticlines in the stratigraphic succession immediately above the Avalon-like basement, at which décollement of the shear zone system was initially rooted. General shear deformation at the ramps involved strain softening with an enhanced component of noncoaxial flow. In contrast, deformation during extrusion in the intervening zones involved strain hardening with a greater component of coaxial flow. Part of the thickening stratigraphic succession exceeded $T_{solidus}$, reflected by the occurrence of migmatites and granites. The latter were partly sourced from the underlying Avalon-like basement that was involved in the deformation and melting. 

## 1. Introduction

Studies of ancient transpressive orogens (e.g. Harland, 1971), and observations at modern convergent plate margins (e.g. Fitch, 1972), suggest that oblique plate motions may lead to slip partitioning, particularly when the plate motion vector is highly oblique to the margin (McCaffrey, 1992; Braun and Beaumont, 1995; Gordon, 1995; Liu et al., 1995; Teyssier et al., 1995). In response, geological structures at all scales are produced by non-steady state flow and heterogeneous deformation (e.g. Tikoff and Fossen, 1993; Jiang, 1994; Fossen and Tikoff, 1997). Heterogeneous deformation involves the development of instabilities, which commonly leads to strain localization in a rock mass (e.g. Ramsay and Graham, 1970; Elliott, 1972; Means et al., 1980; Lister and Williams, 1983; Robin and Cruden, 1994; Jones and Tanner, 1995; Royden, 1996; Zhang et al., 1996; Jiang and Williams, 1998; Burg, 1999). In theory, simple shear is likely to be more localized than pure shear (Cobbold, 1976; see also Lin et al., 1998), because simple shear/noncoaxial strain may lead to strain-softening, whereas pure shear/coaxial strain may lead to strain-hardening (Williams and Price, 1990).

Although many high strain zones in the shallow crust are interpreted to have formed by localized simple shear flow, other flow regimes may operate in the metamorphic environment, that involve deforming wall rocks in high strain zones (Tikoff and Fossen, 1999). If shear is oblique to the principal stretching directions of the wall rocks of a high strain zone, then the deformation path is triclinic and the geometry of the resulting fabric elements is different from those produced by monoclinic deformation (Robin and Cruden, 1994; Jiang and Williams, 1998; Lin et al., 1998). As deformation progresses, strain will be localized by the changing rheology that results from factors such as reaction-enhanced ductility (e.g. White and Knipe, 1978; Rutter and Brodie, 1995) and melting (e.g. Rutter and Neumann, 1995; Brown and Rushmer, 1997; Brown and Solar, 1998a). Further, the introduction of melt into shear zone systems

* Corresponding author. Current address: Department of Earth Sciences, SUNY College at Buffalo, Buffalo, NY 14222, USA. Fax: +1-716-878-4524.

*E-mail address:* solargs@bscmail.buffalostate.edu (G.S. Solar).

0191-8141/01/$ - see front matter 
PII: S0191-8141(00)00175-9

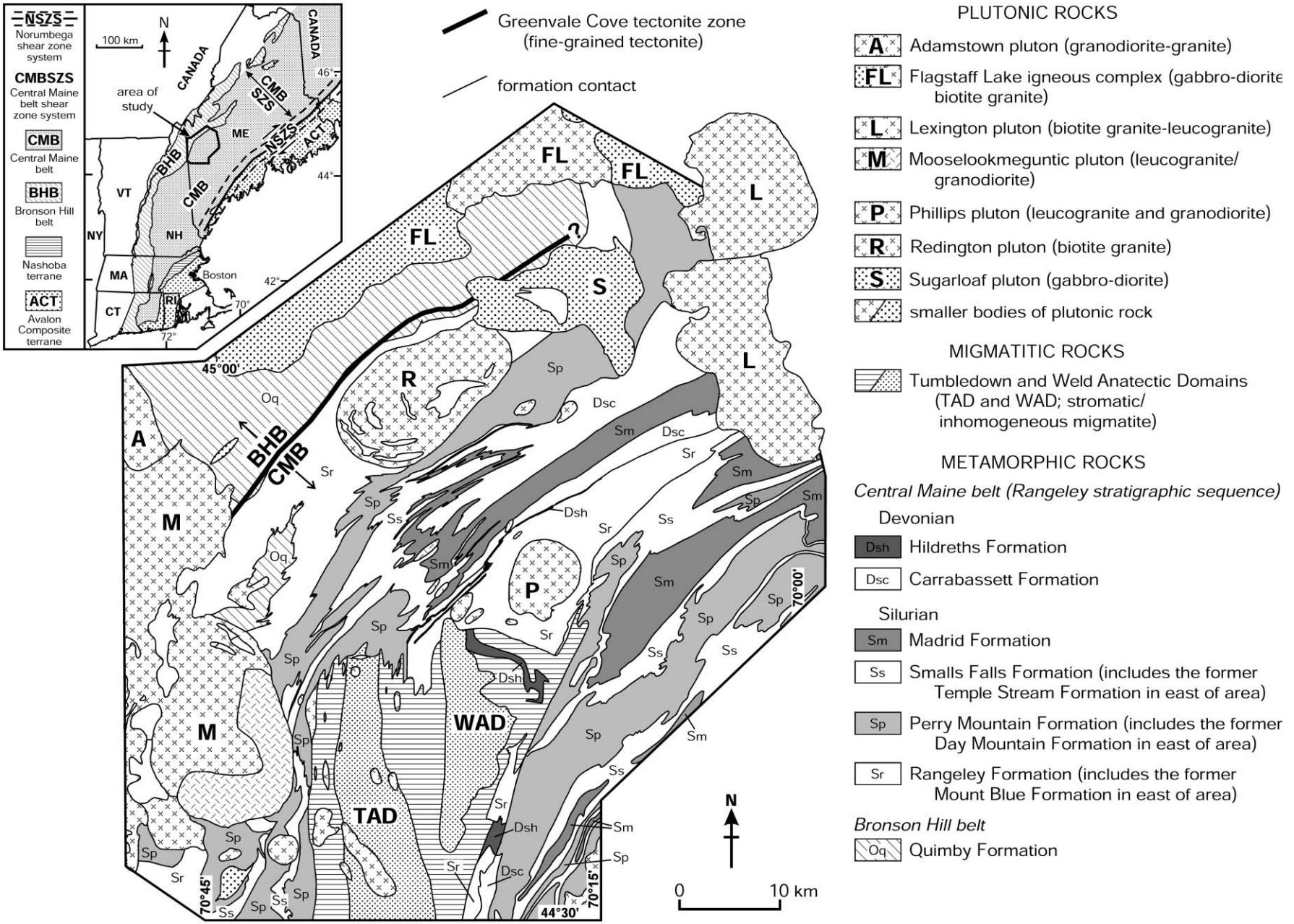
NSZS
Norumbega shear zone system
CMBSZS
Central Maine belt shear zone system
CMB
Central Maine belt
BHB
Bronson Hill belt
Nashoba terrane
ACT
Avalon Composite terrane
100 km
N
CANADA
area of study
ME
VT
NH
NY
MA
CT
RI
Boston
46°
44°
42°
70°
72°
Greenvale Cove tectonite zone (fine-grained tectonite)
formation contact
45°00'
70°45'
70°15'
70°00'
44°30'
0
10 km
PLUTONIC ROCKS
A Adamstown pluton (granodiorite-granite)
FL Flagstaff Lake igneous complex (gabbro-diorite biotite granite)
L Lexington pluton (biotite granite-leucogranite)
M Mooselookmeguntic pluton (leucogranite/ granodiorite)
P Phillips pluton (leucogranite and granodiorite)
R Redington pluton (biotite granite)
S Sugarloaf pluton (gabbro-diorite)
smaller bodies of plutonic rock
MIGMATITIC ROCKS
Tumbledown and Weld Anatectic Domains (TAD and WAD; stromatic/ inhomogeneous migmatite)
METAMORPHIC ROCKS
Central Maine belt (Rangeley stratigraphic sequence)
Devonian
Dsh Hildreths Formation
Dsc Carrabassett Formation
Silurian
Sm Madrid Formation
Ss Smalls Falls Formation (includes the former Temple Stream Formation in east of area)
Sp Perry Mountain Formation (includes the former Day Mountain Formation in east of area)
Sr Rangeley Formation (includes the former Mount Blue Formation in east of area)
Bronson Hill belt
Oq Quimby Formation

is widely postulated as a weakening mechanism that will concentrate strain within the system (Hollister and Crawford, 1986; D'Lemos et al., 1992; Grocott et al., 1994; Pavlis, 1996). Finally, there is the question of the influence of stratigraphic succession as a planar anisotropy on the development of fold belts or thrust belts, particularly with respect to the production of a weak layer due to melting, which will enhance folding over faulting (Erickson, 1996).

Structures in the Central Maine belt of the northern Appalachians (Fig. 1) developed in response to dextral transpression associated with oblique convergence (e.g. van Staal and de Roo, 1995; West and Hubbard, 1997). In this paper, we have used revised stratigraphic mapping (Solar, 1999), structural field data and microstructural fabric observations from an area in western Maine to investigate the nature of deformation partitioning. We have documented mesostructures, microstructures and asymmetric structures, and their spatial relations, and propose a model to explain the progressive evolution of the transpressive shear zone system in which they occur.

## 2. The northern Appalachian orogen

The northern Appalachians are divided into several NNE–SSW-trending tectonostratigraphic units (Fig. 1; Zen, 1989; Robinson et al., 1998). The Central Maine belt (CMB), which is continuous with the Central Mobile belt in Maritime Canada, is the principal unit that occupies most of the eastern part of New England and New Brunswick. The CMB is composed of a Lower Paleozoic sedimentary succession, deformed and metamorphosed at greenschist to upper amphibolite facies conditions, and intruded by plutons of Devonian age (e.g. Osberg et al., 1968; Williams, 1978; Moench et al., 1995; Bradley, 1998; Robinson et al., 1998; Solar et al., 1998). The CMB is located between Ordovician rocks of the Bronson Hill belt (BHB) to the WNW, which were deformed and metamorphosed during the Ordovician Taconian orogeny (Ratcliffe et al., 1998, and references therein), and Neoproterozoic to Silurian rocks of the Avalon Composite terrane (ACT) to the SSE (e.g. Stewart, 1989; Stewart et al., 1992; West et al., 1995; Cocks et al., 1997).

In the northern Appalachian orogen, deformation was partitioned heterogeneously during dextral transpression in response to Early Devonian oblique convergence (van Staal and de Roo, 1995; van Staal et al., 1998). Dextral–SE-side-up displacement was accommodated within the CMB shear zone system (Brown and Solar, 1998a; Solar et al., 1998; Solar, 1999; Solar and Brown, 1999) while dextral–transcurrent displacement was accommodated within the Norumbega shear zone system (Swanson, 1992; West and Hubbard, 1997; West, 1999) along the southeastern side of the CMB (Fig. 1). By the Carboniferous, deformation had ceased within the CMB shear zone system and strain had localized into the Norumbega shear zone system (Hubbard et al., 1995; West and Hubbard, 1997; Ludman, 1998; West, 1999).

## 3. The geology of western Maine

In eastern New Hampshire and western Maine, interpretations of the structure have concentrated traditionally on the regional scale folds and syn-deposition faults inferred from the map patterns of stratigraphic units (Fig. 1; e.g. Moench, 1970b; Bradley, 1983; Moench and Pankiwskyj, 1988; Moench et al., 1995; Eusden et al., 1996). Much effort has been made to document metamorphic reactions, and to separate periods of metamorphism (e.g. Guidotti, 1974, 1989; Holdaway et al., 1982; Chamberlain and England, 1985; Eusden and Barreiro, 1988; Smith and Barreiro, 1990) and plutonism (e.g. Tomascak et al., 1996; Bradley, 1998; Solar et al., 1998).

### 3.1. The Rangeley stratigraphic sequence

The CMB is composed of a Silurian to Early Devonian sedimentary succession called the "Rangeley stratigraphic sequence" that was deformed and metamorphosed during the Devonian (Acadian orogeny; Bradley, 1998). The sequence is estimated to be as much as 10 km in thickness, made up of ~5 km each of Silurian and Devonian rocks (Moench and Boudette, 1970; Moench et al., 1995). Stratigraphic units are defined in the western Maine study area (Fig. 1; Moench and Boudette, 1970), and have been extended across most of the New England Appalachians (e.g. Hatch et al., 1983).

The stratigraphy of the sequence is preserved through metamorphism, and begins in the northwest with a proximal coarse conglomerate in the lower part of the Rangeley Formation, interpreted to mark the beginning of the Silurian (e.g. Moench, 1970a), grades upward (SE) into a progressively distal Silurian turbidite sequence and finishes in the central part of the area (Fig. 1) with a distal Devonian unit (see Moench et al., 1995, for a summary). The sequence has

Fig. 1. Geological map of the study area, western Maine. Devonian transpression (Acadian orogeny) was partitioned into oblique thrusting (dextral) in the Central Maine belt shear zone system (CMBSZS) and dextral–transcurrent displacement along the Norumbega shear zone system (NSZS). CT = Connecticut, NH = New Hampshire, MA = Massachusetts, ME = Maine, RI = Rhode Island, and VT = Vermont. The map pattern of stratigraphic units in the study area is modified from Moench et al. (1995), based on new mapping and interpretation of existing maps (Solar, 1999). Within the Rangeley stratigraphic sequence, alternate units are shaded to clarify the map pattern of the stratigraphic succession. Structures in this map area are shown in Figs. 2 and 3. BHB is the Bronson Hill belt and CMB is the Central Maine belt. The Greenvale Cove tectonite zone coincides in part with the map pattern of the Greenvale Cove Formation of Moench (1969, 1971) and Moench et al. (1995).

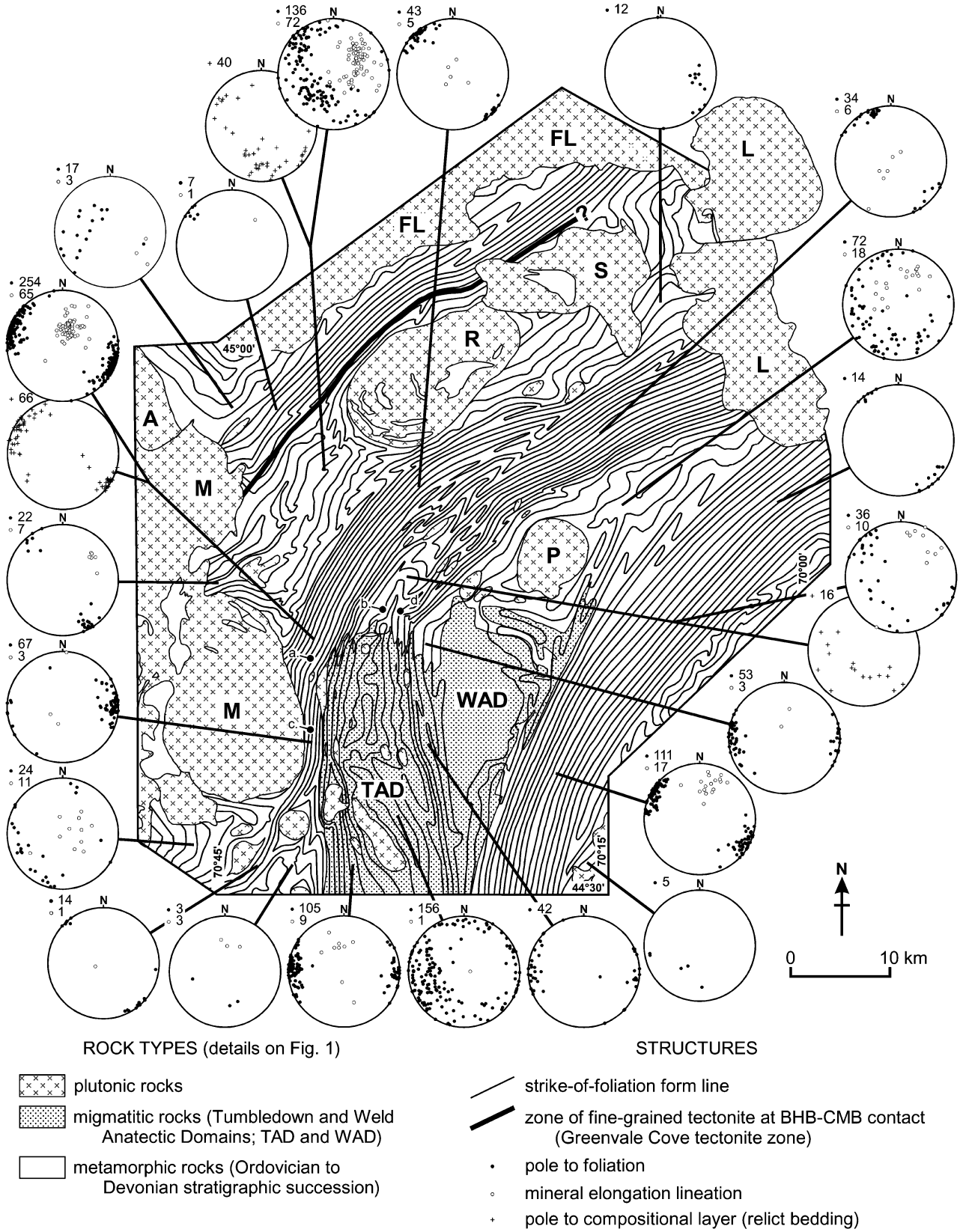


Fig. 2. Form line map of foliation in the study area (modified after Brown and Solar, 1998b; Solar, 1999). More closely-spaced lines denote steep foliation dips and more widely-spaced lines denote moderate dips; foliation is only locally shallowly dipping. Continuous belts of steeply-dipping, N- to NE-striking foliation ('straight' belts) alternate with intervening zones where foliation has moderate dips and variable strike (see text for details). Stereograms are lower-hemisphere, equal-area (Schmidt) projections of grain-shape fabrics, and poles to compositional layers measured in the field. Since the structural system is curved at the regional scale, structural data rotate from NE–SW trends in the NE to N–S in the SW. The structural pattern rotates back to NE–SW along strike to the SW out of the study area. Orientation of compositional layering and foliation for outcrops at (a), (b), (c) and (d) are shown in Fig. 3.

been separated into seven apparently conformable formations, based largely on the relative thickness and frequency of alternating centimeter- to decimeter-scale psammite vs pelite layers (inferred relict bedding; Moench, 1970a; Moench and Boudette, 1970), coupled with variations in the proportion of metamorphic minerals in the pelite layers (Moench, 1998, personal communication). Locally, cross-stratification is preserved in psammite layers (particularly in the Perry Mountain Formation).The summary stratigraphic succession listed in Fig. 1 follows the most recent compilation of Moench et al. (1995), but is modified in the eastern part of the study area (Solar, 1999).

### 3.2. Regional metamorphism

Polymetamorphism of the Rangeley stratigraphic sequence in western Maine is well documented, particularly regarding the rocks to the northwest and east of the migmatite domains, TAD and WAD (Guidotti, 1970, 1974, 1989; Holdaway et al., 1982, 1997). The study area is located in the part of Maine where greenschist facies rocks to the northeast increase in grade to upper amphibolite facies within 20 km along strike to the southwest (see summary in Guidotti, 1989). Across the study area, the amphibolite facies rocks are characterized by porphyroblasts of garnet, staurolite and locally pseudomorphed andalusite enclosed within a matrix dominated by muscovite, biotite, quartz, plagioclase, and opaque phases, generally ilmenite, graphite and pyrite. Fibrolite is an important fabric-forming matrix phase at upper amphibolite facies, especially in migmatitic rocks. Thus, the metamorphism is of high-*T*–low-*P* type, although the metamorphic field gradient is the product of polymetamorphism (e.g. Guidotti, 1989) related to pluton-driven thermal pulses (De Yoreo et al., 1991) overprinted on a regionally elevated thermal gradient that resulted from transpression (Brown and Solar, 1999; Solar and Brown, 1999).

### 3.3. Migmatite

Within the CMB, the study area marks the northern limit of migmatite in the northern Appalachians, in the Tumbledown and Weld anatectic domains (TAD and WAD), respectively (Fig. 1). In western Maine, we separate migmatites into stromatic and inhomogeneous varieties (e.g. Brown and Solar, 1999). These two types of migmatite map into discrete zones that alternate across the regional strike (Fig. 1), and are interpreted to have formed at similar structural levels (Solar, 1999). The protolith of the migmatites is interpreted to be rocks of the Rangeley stratigraphic sequence based upon compositional layers that reflect relict bedding in some of these rocks, and because the mineral assemblage of sillimanite (fibrolite) + garnet + biotite + quartz + plagioclase + opaque phases ± muscovite ± clinozoisite is consistent with metamorphism of psammite and pelite at upper amphibolite facies conditions. All migmatites contain fibrolite and biotite as the fabric-forming phases, and have discrete to diffuse leucosomes containing microstructures, such as crystal faces and mineral films along grain boundaries, consistent with crystallization from melt (e.g. Sawyer, 1999).

The stromatic migmatites have a planar structure defined by parallel centimeter-scale compositional layers, penetrative foliation and high-aspect-ratio leucosomes. Centimeter- to meter-thick granite sheets are concordant to weakly discordant with respect to the planar structures. Many of these sheets are composite (Brown and Solar, 1999). Inhomogeneous migmatite lacks this planar structure, and includes several different structural types whose contacts are gradational (Solar, 1999). In the northern part of the TAD and WAD, leucosomes in diatexite migmatites are diffuse to discrete, in which case the leucosomes tend to be rod-shaped with a long dimension that is moderately-to-steeply ENE plunging, similar to the attitude of mineral elongation lineation. Meter-scale cylindrical bodies of granite occur within these diatexite migmatites. We have argued that melt was pumped along the foliation in the stromatic migmatite, while en masse transfer of melt plus residue by melt-enhanced granular flow occurred in the inhomogeneous migmatite (Brown and Solar, 1998a,b, 1999).

### 3.4. Granite

Granite plutons are kilometer-scale by area (Fig. 1). In contrast to country rocks, the granites record no evidence of solid-state deformation internally, although foliation is apparently deflected in rocks around the Redington pluton (R; Figs. 1 and 2). Some larger plutons cut across the regional structures without either significant deflection of structural trends or formation of a significant deformation aureole (Figs. 1 and 2), suggesting displacement of rock out of the map plane. The close association between smaller plutons (by area), such as the Phillips pluton, the Lexington pluton in its northern part, and inhomogeneous migmatite in similar structural zones (Figs. 1 and 2), has been used to suggest a relationship between structure, granite ascent and emplacement (Brown and Solar, 1998a, 1998b, 1999; Pressley and Brown, 1999).

### 3.5. Timing of orogenesis

Smith and Barreiro (1990) determined U–Pb monazite ages from samples of pelite collected from staurolite zone rocks. Their results demonstrate two distinct concentrations of metamorphic ages that are interpreted to reflect regional metamorphism at 405–399 ± 2 Ma and contact metamorphism related to the Mooselookmeguntic pluton (Figs. 1 and 2) at 369–363 ± 2 Ma. Solar et al. (1998) determined U–Pb zircon and monazite ages (interpreted to date crystallization) from samples of granite sheets and lenses in stromatic migmatite, and plutons. These ages are concordant, and are similar in the range c. 408–404 Ma, except the younger Mooselookmeguntic pluton, which yielded ages of c. 389 and c. 370 Ma from two discrete

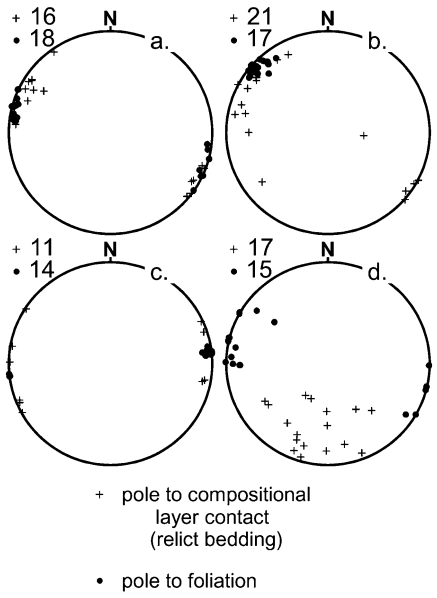


Fig. 3. Lower-hemisphere, equal-area (Schmidt) projections of grain-shape fabrics (defined by bladed mica and elongate ribbons of quartz aggregates) and poles to compositional layers for four outcrops: (a) and (c) are from 'straight' belt rocks, (b) is from a structural transition zone and (d) is from rocks in an intervening zone. Locations are shown in Fig. 2. There is a strong similarity in orientation of both compositional layering and foliation in 'straight' belts, which is not seen in the outcrop from the intervening zone.

granite types. These data support a model of contemporaneous deformation, metamorphism, and granite ascent through the crust in the study area (Brown and Solar, 1999).

## 4. Structural geology of western Maine

### *4.1. Two types of structural zone*

The principal structures of western Maine are: (1) the kilometer scale open to tight folds of the stratigraphic succession, defined by the orientation of centimeter to decimeter scale psammite–pelite compositional layers (Fig. 1; see Fig. 4, section A–A′); and, (2) the kilometer scale alternation of structural zones, defined by the NE–SW-striking and steeply SE dipping domainal structure of the CMB shear zone system and the characteristic fabrics of the alternating zones (Figs. 2 and 3; Solar and Brown, 1999). The regional structure is well illustrated by the foliation form line map of Fig. 2, in which a pattern emerges of zones of straight and sub-parallel form lines that wrap around areas where the form lines are more variable in strike. These two types of structural zone coincide with differences in the dip of compositional layers; the layers are more steeply dipping in the zones of straight foliation form lines. The structural style and intensity of fabrics in each of these zones vary with compositional layer and metamorphic grade (Solar and Brown, 1999).

Stereograms of the attitudes of mineral fabrics and compositional layers (Fig. 2) show the fundamental difference between each zone. A strong NE-plunging penetrative mineral elongation lineation (amount of plunge variable) is present in metasedimentary rocks in both types of zone, and is defined by the same metamorphic minerals at the same metamorphic grade. In contrast, the intensity and orientation of foliation vary by zone. Where foliation form lines are sub-parallel, foliation is strongly developed, and is oriented sub-parallel to contacts between compositional layers (Figs. 2 and 3). This structural style occurs in 'straight' to arcuate belts at outcrop and map scales (Fig. 2). In contrast, rocks in the intervening zones between these 'straight' belts have weakly-defined foliation that is variable in orientation. Further, compositional layers in the intervening zones vary in attitude, and are not parallel to foliation in the same outcrop (Fig. 3), which transects the layers. At map-scale, the pattern of structural zones shows an alternation of these two types such that 'straight' belts of consistently-oriented planar structures, some of which anastomose, are separated by intervening zones, some of which are lens-shaped, in which planar structures vary in orientation (Fig. 2).

Boundaries between the structural zones appear sharp at map scale (Fig. 2), but are gradational in outcrop over meter-scale transition zones. Across these transitions, traversing away from 'straight' belts into the intervening zone rocks, compositional layers and foliation change progressively, becoming more variable in strike and more moderate in dip. However, the orientations of both mineral lineations and hinge lines of folded compositional layers generally do not vary significantly across these transitions. Foliation diminishes in intensity in the same direction, away from the 'straight' belts, but the lineation is equally well developed in both zones, with a progressively more variable attitude (Fig. 2, stereograms). Contacts between stratigraphic units generally occur within these structural transition zones, as do the transitions between stromatic and inhomogeneous migmatite types, but at map-scale lithological contacts are transected at a shallow angle by structural zone boundaries (compare Figs. 1 and 2). Also, styles of migmatite (summarized by Solar, 1999) and shapes of granite bodies within the migmatite domains (TAD and WAD; Brown and Solar, 1999) vary consistently with structural zone, where stromatic migmatite and sheets of granite are largely within 'straight' belts, while inhomogeneous migmatite and cylinders of granite occur exclusively within intervening zones (Figs. 1 and 2).

### *4.2. Three-dimensional structure of the CMB shear zone system*

Our model of the three-dimensional structure of western Maine is based upon the mapped structural pattern and interpretations of various types of geophysical data on the subsurface structure (Stewart, 1989; Unger et al., 1989; Stewart et al., 1992; Zhu and Ebel, 1994; Musacchio et al.,

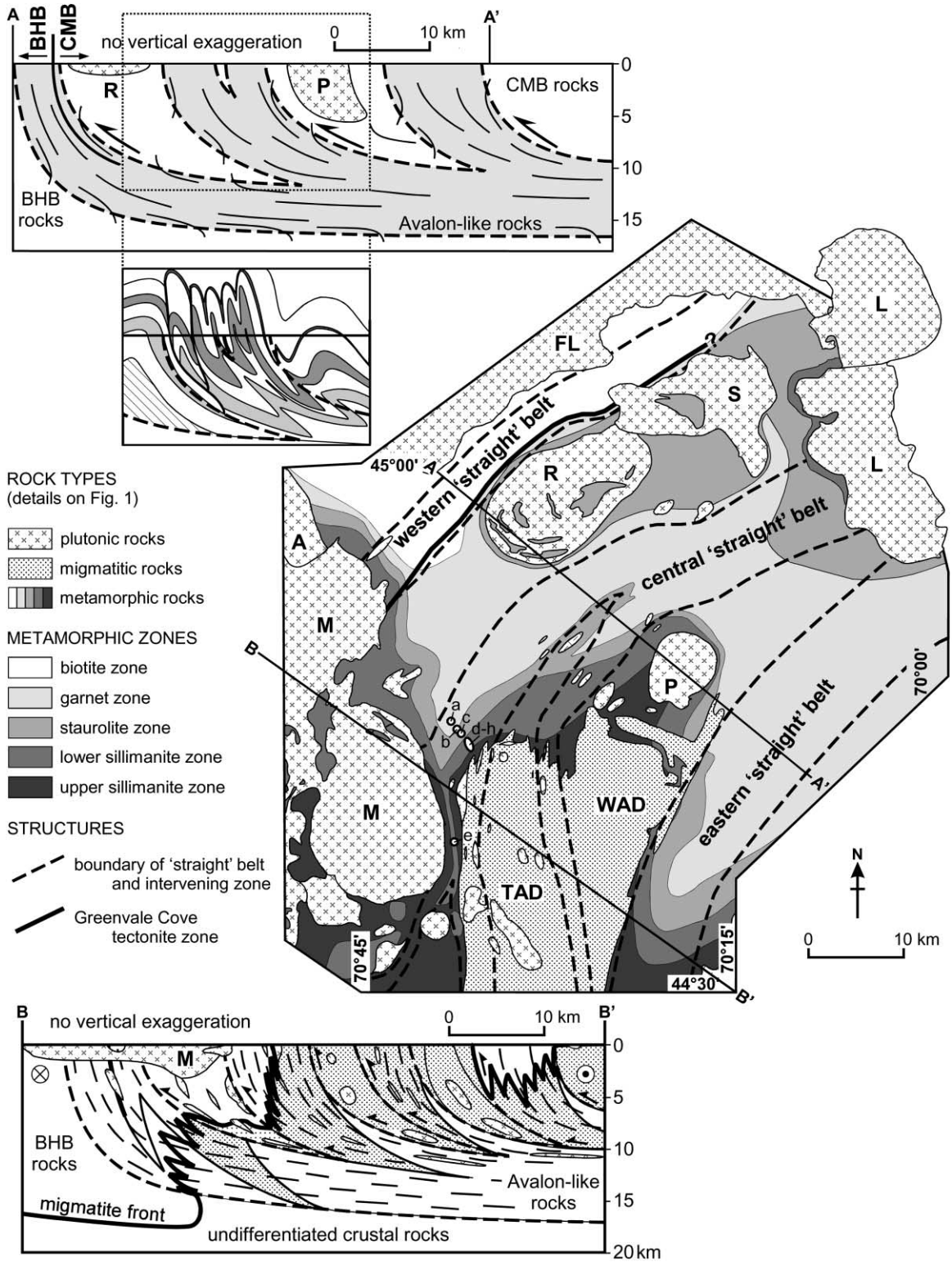


Fig. 4. Simplified structural and metamorphic zone map and structure sections. The locations of 'straight' belts are indicated. $S_i$–$S_e$ rakes shown in Fig. 8 are from locations a–i. Section A–A′ shows the inferred listric geometry of the structural system where 'straight' belts (shaded) converge into a single shallowly SE-dipping root zone at ~13 km depth (Brown and Solar, 1999). Line segments on A–A′ are intersections of mineral foliation with the plane of the diagram. The curvature of foliation across boundaries between structural zones is intended to show SE-side-up sense of shear. The area within the dotted line box on A–A′ is shown below the section to illustrate the inferred geometry of folds of the stratigraphic sequence (tighter in 'straight' belts; ornament is the same as shown on Fig. 1). Section B–B′ is drawn to show the higher-grade rocks, particularly the inferred distribution of migmatites with depth (see Brown and Solar, 1999; Solar, 1999). Line segments are intersections of foliation with the plane of section. Avalon-like basement rocks are thrust imbricately westward to thicken the crust. Following thickening, isotherms are displaced upward in the crust as illustrated by the asymmetric migmatite front (the contemporary solidus, shown as a continuous solid line).

1997). From the arc described by the 'straight' belts in the map plane (concave to the SE) and their strike length (Fig. 2), we infer that they continue to depth. Based upon interpretations of geophysical data (Brown and Solar, 1998b), we interpret these zones to converge into a sub-horizontal root zone at approximately 13 km depth (see Fig. 4). Intervening zones are interpreted to pinch out with depth. Toward shallower levels, now removed by erosion, the 'straight' belts may have fanned upward in response to decreasing *T*. Although intervening zones likely thickened upward as the 'straight' belts narrowed to maintain strain compatibility, they also change in three-dimensional geometry from lens-shaped to planar, as reflected in the spatial change from SE to NW from deeper to shallower structural levels. Thus, we interpret the three-dimensional shape of the structure to be listric where dips shallow with increasing depth. This interpretation is consistent with the expected change in orientation of structures as a result of the decrease in supported differential stress with increasing depth, and with the production of a weak layer at depth as part of the stratigraphic succession begins to melt. The steeper plunge of lineations in the central part of the area of study, where the foliation is rotated from NE- to N-striking, may reflect deformation in a restraining bend within the structure. Steeper lineations in the restraining bend may record a larger component of dip-parallel displacement, which may account for the occurrence of migmatite in this area, reflecting exhumation of deeper crust.

### *4.3. 'Straight' belts*

#### *4.3.1. Mesostructures*

Primary structures in 'straight' belt rocks include rhythmic alternation of lithological layers of psammite and pelite

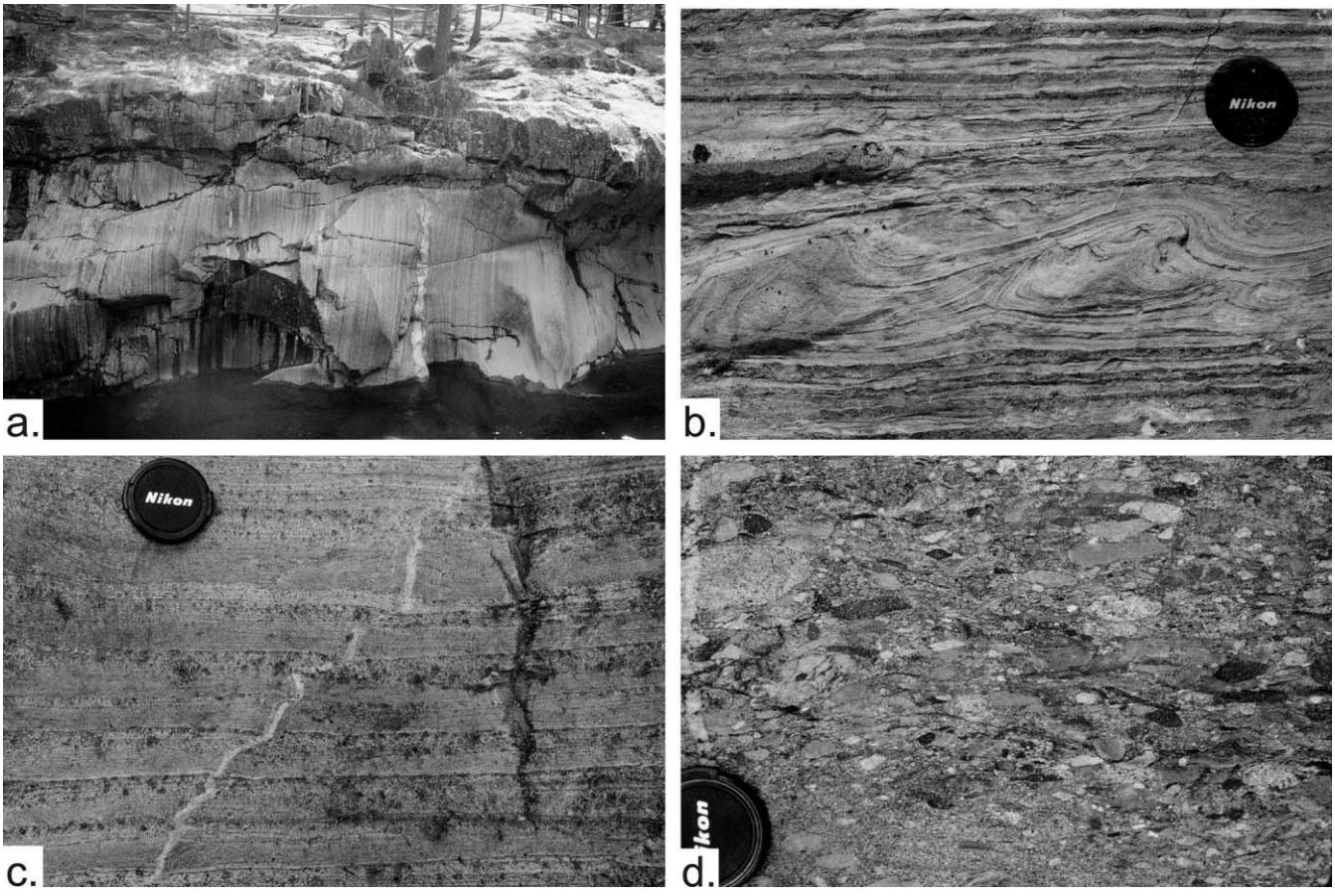


Fig. 5. Field relations in 'straight' belts. (a) Steep exposure of Perry Mountain Formation in the central 'straight' belt, as seen in the Swift River (Coos Canyon), Byron, Maine. View is along strike of the compositional layers to the SSW (ESE is left). The alternating layers with different gray intensities reflect differences in composition (lighter gray is psammite, darker gray is pelite). Note the 'pinch and swell' structure of the granite sheet at right of center, which is sub-parallel to layering, and the boudinaged granite sheet at left of center, which is discordant to layering. (b) Preserved waveform stratigraphy in the Perry Mountain Formation at the type locality on Perry Mountain in Sandy River Plantation, Maine (central 'straight' belt). In views down-plunge of the mineral elongation lineation, these structures are always tilted to the right (NE) along the layering, consistent with other kinematic indicators (see Fig. 6). (c) Pavement exposure of compositional layers in Perry Mountain Formation (central 'straight' belt; Coos Canyon, Byron, Maine) that illustrate dextral general shear. The quartz vein is sheared inhomogeneously to the right along the compositional layers; shear was concentrated within the pelite layers (darker gray layers). The psammite layer immediately below the lens cap has its greatest thickness where it is cut by the quartz vein to indicate flattening across the compositional layers. Sense of shear is consistent with other kinematic indicators (see Fig. 6). (d) Flattened conglomerate in the basal Rangeley Formation [unit 'a' of Moench et al. (1995)] at the type locality, western 'straight' belt, Maine Rt. 4, SE of Rangeley, Maine.

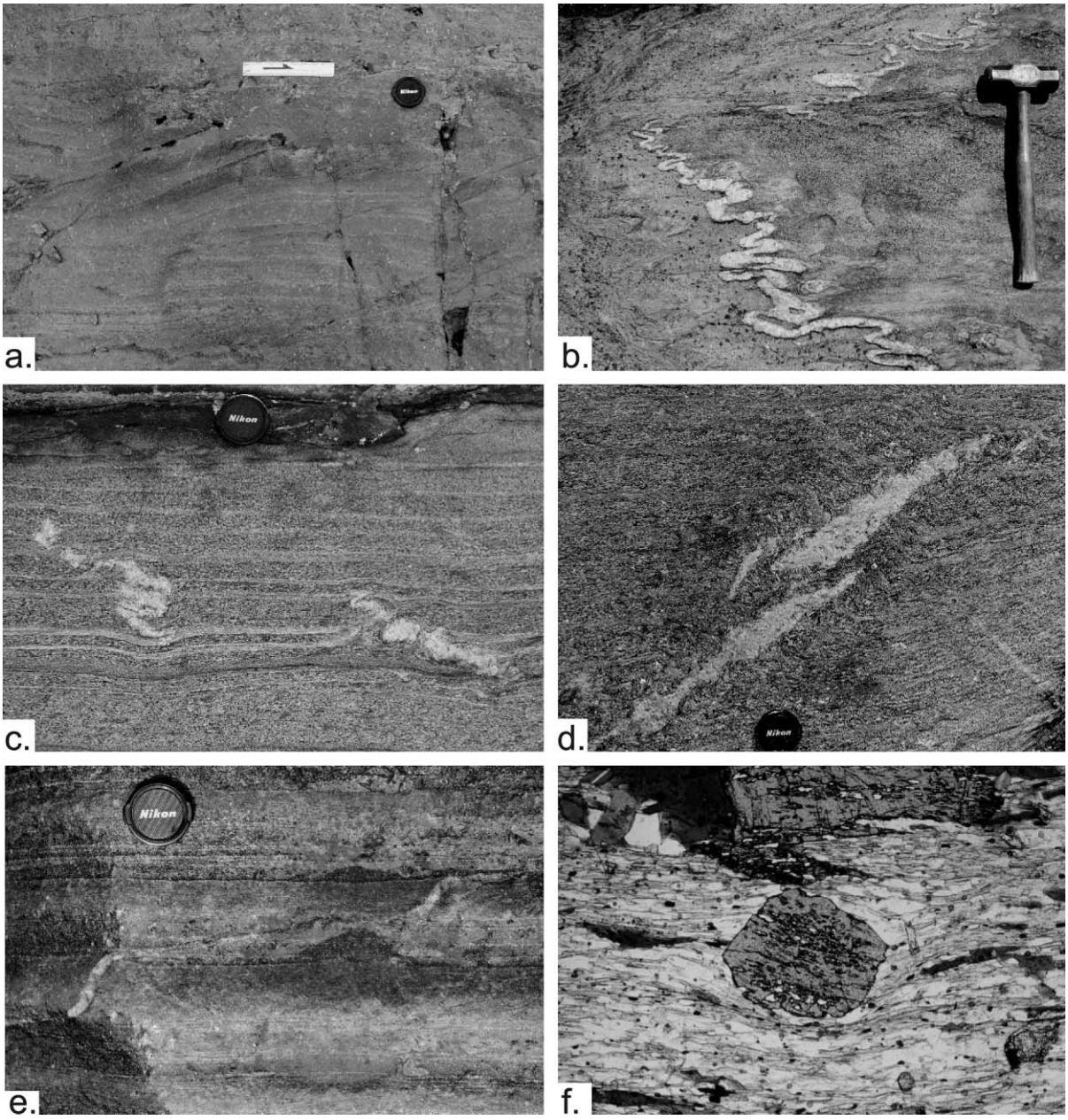


Fig. 6. Asymmetric structures in 'straight' belt rocks that suggest dextral–SE-side-up sense of shear. (a) Dextral ramps of compositional layers in pavement exposure of the Rangeley Formation (western 'straight' belt), near Rangeley, Maine. (b) Quartz vein parallel to compositional layers folded parasitically (Perry Mountain Formation, central 'straight belt'), Swift River, Byron, Maine. Note dextral shear of the hinge zone (upper left). (c and d) Ptygmatic folds of discordant granite (c) and granite in shear fractures (d) in the same set of layers in pavement outcrop of high grade (upper amphibolite facies) Perry Mountain Formation, Swift River, Mexico, Maine. Each structure is interpreted to indicate dextral shear, because the folds in (c) are the result of shortening of left-stepping tension gashes during layer-parallel shear and layer-normal flattening, and the veins in (d) are interpreted to infill brittle shears formed in association with cm-scale folds of the foliation. (e) Sheared quartz vein in pavement outcrop of the Perry Mountain Formation (central 'straight' belt), Byron, Maine. The vein is interpreted to have formed sub-perpendicularly to layers, but subsequently underwent inhomogeneous dextral shear. Shear was apparently localized within the pelite layers (as in Fig. 5c). (f) Asymmetric microstructure in lineation parallel and foliation perpendicular thin section view (long dimension is 3.5 mm), sample of Perry Mountain Formation, Swift River, N of Byron, Maine. The garnet porphyroblast has quartz and mica strain shadows that resemble $\sigma$ tails to suggest top-to-the-right sense of shear. This suggests shear was along the foliation in the direction of the lineation. In this view SE is to the top, so shear was SE-side up along the lineation. The inclusion trails in the garnet are not parallel to matrix foliation (see rake data in Fig. 8).

(Figs. 5 and 6). Locally, cross-lamination, asymmetric ripples and convolute lamination are preserved within psammite layers. Ripple patterns when observed show interference of the initial waveform and folding, that accentuates the asymmetry of these sedimentary structures (Fig. 5b). On a strictly local basis, stratigraphic way up may be determined, particularly where cross-laminae and ripples are observed in psammite. Using these local structures,

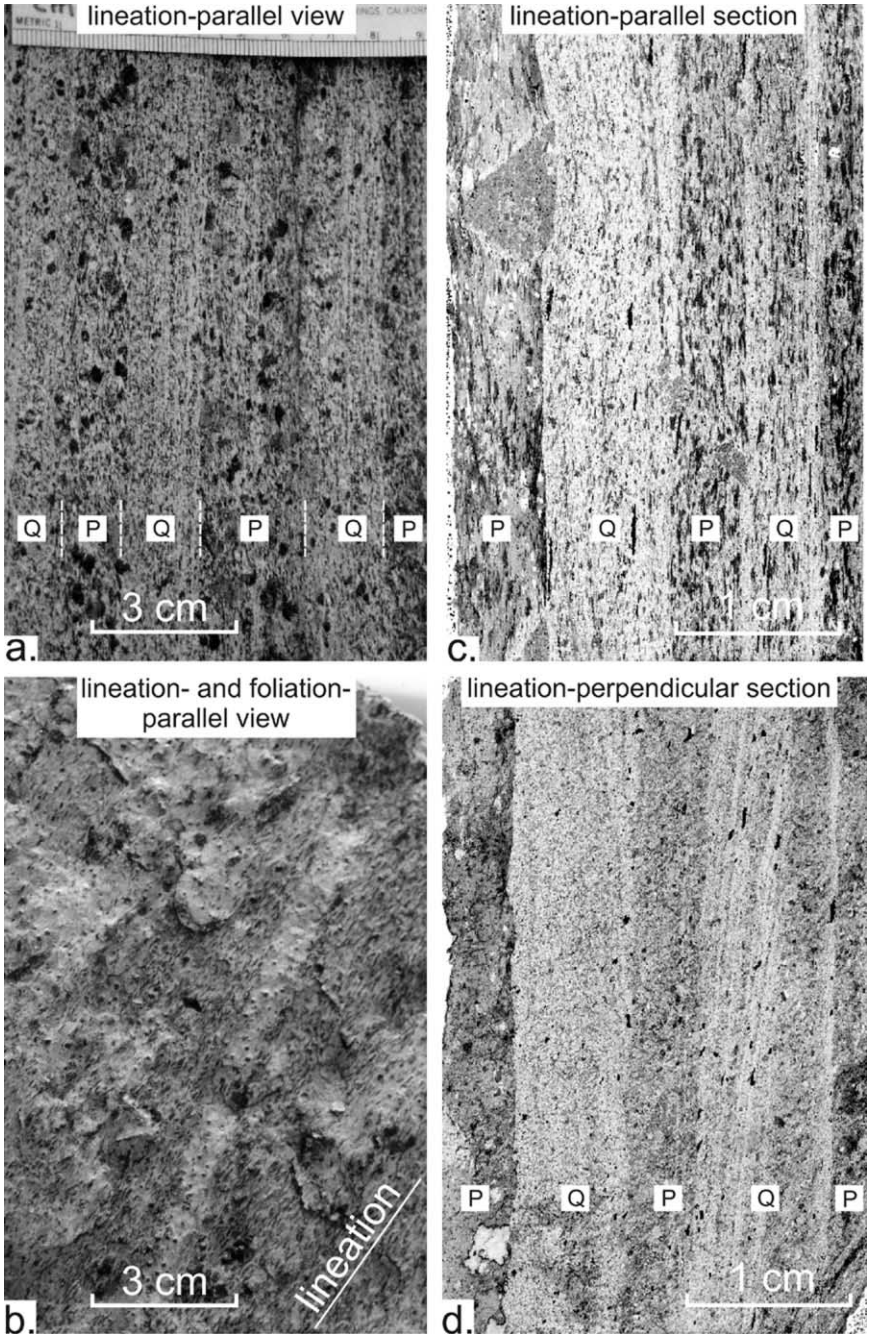


Fig. 7. A pair of field photographs (a and b) and a pair of transmitted light photomicrographs of thin sections cut perpendicular to foliation (c and d) that show typical microstructural relations in 'straight' belt rocks, both pairs from the Perry Mountain Formation in the central 'straight' belt, Byron, Maine. The thin section pair is from the rock shown in (a) and (b), and consists of a lineation-parallel view (c) and a perpendicular view, downplunge of the lineation (d). Q and P mark the centers of quartzo–feldspathic and pelite domains (Q- and P-domains), respectively. These are mineral segregation layers whose intensity varies along their length, and are scale dependent [compare (a) and (c)]. Contacts between these domains are sharp. (a) View parallel to lineation and perpendicular to foliation (view down to the SW, SE is to the left, lineation plunge is downward in the plane of the page). (b) View parallel to both lineation and foliation (NE is to the left). The mineral fabric is strongly developed and defined by the preferred orientation of elongate muscovite and acicular biotite porphyroblasts. In (c), biotite porphyroblasts are 'fish', and porphyroblasts of staurolite are wrapped by matrix minerals to form strain-shadow tails along the lineation. Some of these tails are asymmetric suggesting left-side (SE-side) up shear sense along the lineation. In (b), the pseudomorph after andalusite is elongate along the foliation, at a shallow angle to the lineation. Comparison of lineation-parallel and lineation-perpendicular views illustrates the penetrative nature of foliation and lineation, where grain shapes are conspicuously longer in the lineation-parallel view. In (c), the strain shadow tails around porphyroblasts of staurolite, garnet and biotite are pronounced relative to these structures in (d).

younging is generally toward the southeast across strike. Without these features, establishing way up is difficult because sharp contacts occur on both sides of compositional layers making the use of apparent relict grading problematic. In pelite layers, sedimentary structures have not been preserved due to recrystallization and the development of a pronounced centimeter-scale mineral segregation fabric of alternating quartzo–feldspathic (Q) and mica-rich/pelite (P) domains (cf. Passchier and Trouw, 1996; see also Yardley, 1989), sub-parallel to psammite–pelite contacts. This domainal fabric resembles sedimentary bedding due to sharp contacts across strike (Figs. 5 and 7; see also Solar and Brown, 1999), but the domains are gradational along strike (Fig. 7a). Since all rocks considered here are recrystallized, most at amphibolite facies conditions, we expect that primary millimeter scale sedimentary lamination will no longer be preserved. Thus, the determination of stratigraphic way up based upon apparent grain-size sorting and grading is unlikely to be reliable at this (millimeter) scale where grain size reflects recrystallization and/or recorded strain. Thinning of compositional layers is evident (e.g. Fig. 5c) by the presence of flattened and elongated cobbles in conglomerate of the basal Rangeley Formation (Fig. 5d) and elongated pods of calc-silicate rock (relict concretions) found throughout the succession. Matrix fabrics are truncated and/or are flattened against porphyroblasts of staurolite where they occur at psammite-pelite contacts (Solar, 1999; Solar and Brown, 1999).

Compositional layers are typically centimeter scale and laterally continuous. Layers are planar and sub-parallel, and therefore form a ‘straight’ structure in all two-dimensional views (Figs. 5 and 6), and a planar structure in three-dimensions (see stereograms in Fig. 2). Local contortion of layers into tight meter-scale asymmetric folds occurs within discrete and isolated meter-scale domains at outcrop (Fig. 6). In the same outcrops, folds form both ‘Z’- and ‘S’-asymmetries in down-plunge profile view, all with moderately NE-plunging hinge lines. Generally, layers in the short limb of ‘Z’ folds are thinner in comparison with the same layer in the long limb. In contrast, layers in the short limb of ‘S’ folds commonly are thicker, but in both cases, compositional layers in the longer limbs are oriented parallel to non-folded layers in the same outcrop. Shapes of folds at their hinge zones are angular to sub-rounded, with the more rounded hinge zones defined by psammite layers. Typically, meter-scale folds are disharmonic to polyharmonic with apparent parasitic centimeter and millimeter scale folds of mineral segregation layers within pelite layers, indicating that metamorphic segregation to form the Q and P domains occurred pre- to syn-folding. The orientation of hinge lines of these folds is sub-parallel across the ‘straight’ belts, but varies along strike such that they are more steeply NE-plunging in the south, and more shallowly NE-plunging in the north. Foliation in the meter-scale fold domains transects fold limbs without disruption, and is not parallel to the fold axial plane. The foliation is continuous with the penetrative foliation in the outcrop. Without any supporting evidence of overprinting, we interpret these variations in plunge of fold hinge lines and foliation-transected folds to have been produced during one progressive triclinic deformation (cf. Jiang and Williams, 1998). Locally, quartz veins are associated with folds, and deformed as part of the fold set (e.g. Fig. 6b), or quartz veins occur as tension gashes within fold hinge zones in psammite only.

In outcrops, typical asymmetric structures are: (1) decimeter-scale zones of disrupted and thickened compositional layers (Fig. 6a); (2) offset quartz veins (Figs. 5c and 6b and e); (3) en echelon ptygmatic folds of quartz veins (Fig. 6c); (4) centimeter- and millimeter-scale en echelon quartz or granite filled shear fractures (Fig. 6d); (5) en echelon mineralized tension gashes in psammite layers; (6) discordant decimeter- and centimeter-scale quartz and granite boudinage and ‘pinch-and-swell’ structures (Figs. 5a and 6e); and (7) asymmetric tails wrapped around porphyroblasts of garnet and staurolite. Commonly, millimeter-scale en echelon veins truncate mineral fabrics, and are limited to psammite layers, whereas centimeter-scale veins refract across layer contacts in staurolite grade rocks (e.g. Fig. 6e), and cross centimeter scale layers at sillimanite grade (e.g. Fig. 6c and d). In horizontal view, en echelon quartz- or granite-filled shear fractures are consistently right stepping across strike while mineralized tension gashes consistently step left. In vertical views to the SW, these same en echelon structures are up and down stepping, respectively. In pavement, both centimeter-scale discordant boudinage and zones of thickened strata are offset consistently right lateral (Fig. 6a) while in vertical views to the SW these structures are consistently SE-side-up offset across the ‘straight’ belts (Fig. 5a).

At the millimeter scale, rocks are typified by a penetrative steeply SE-dipping mica and quartz-ribbon foliation and a moderately NE-plunging bladed muscovite and acicular biotite mineral elongation lineation (Fig. 7a and b). Foliation is straight and oriented consistently with steep dips in all two-dimensional views to define a planar fabric similar in attitude to contacts between compositional layers. Attitudes of the mineral fabric do not vary more than 2° in any direction across a meter scale outcrop, or 5° across larger outcrops (Fig. 5a).

Fabrics in greenschist and lower amphibolite facies rocks are typified by a pronounced cleavage overprinted upon apparent relict convolute bedding (Guidotti, 1974; Solar, 1999). Foliation in pelite layers is typically discordant to compositional layers (5–10°). At middle amphibolite facies, biotite occurs as ‘fish’. Aggregates of quartz that form strain shadow tails around porphyroblasts of staurolite and pseudomorphs after andalusite are locally conspicuous in outcrop (Solar and Brown, 1999). Foliation is locally crenulated at the centimeter-scale with moderately NE-plunging hinge lines. An intersection lineation is defined within some of these rocks by the intersection of the dominant mica foliation, seen in Fig. 7a,c and d, and a weaker spaced biotite

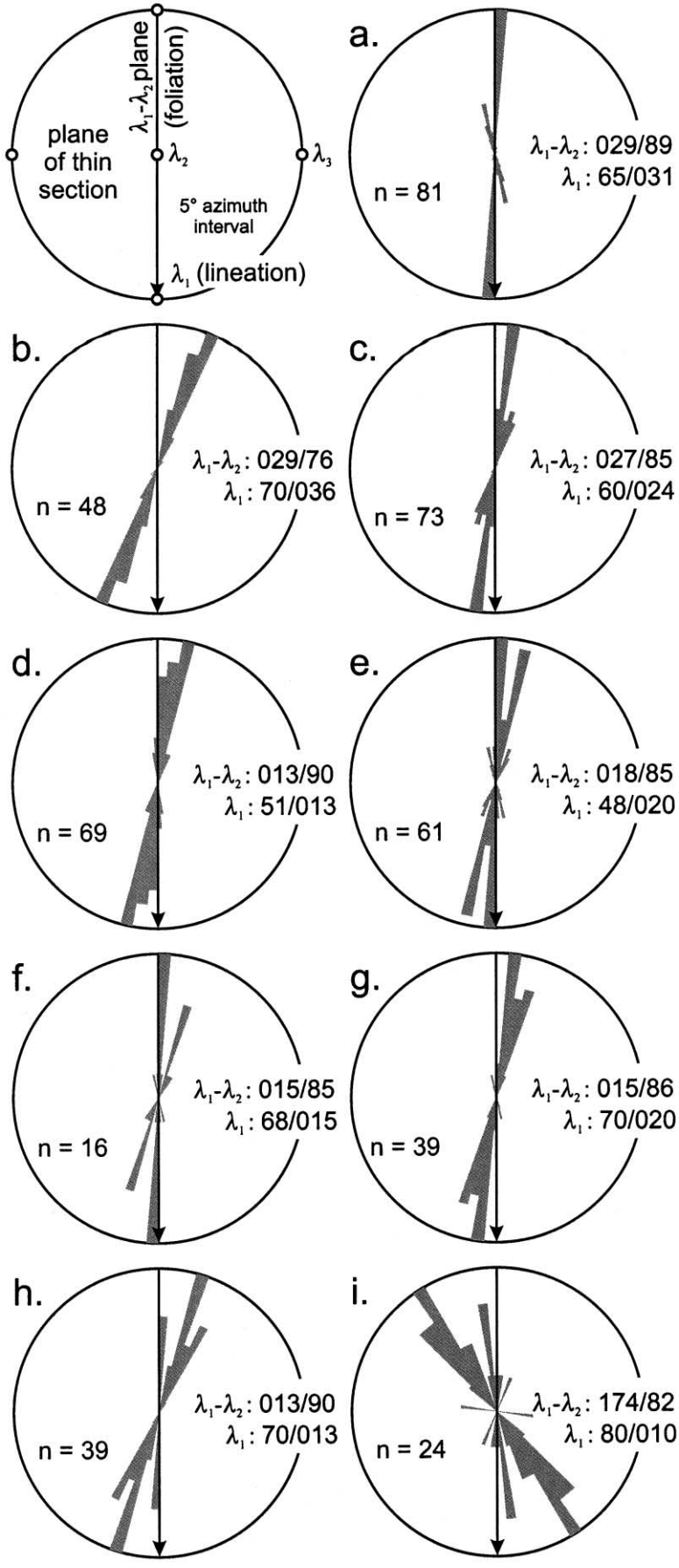
λ1-λ2 plane (foliation)
plane of thin section
λ2
λ3
5° azimuth interval
λ1 (lineation)
a.
n = 81
λ1-λ2: 029/89
λ1: 65/031
b.
n = 48
λ1-λ2: 029/76
λ1: 70/036
c.
n = 73
λ1-λ2: 027/85
λ1: 60/024
d.
n = 69
λ1-λ2: 013/90
λ1: 51/013
e.
n = 61
λ1-λ2: 018/85
λ1: 48/020
f.
n = 16
λ1-λ2: 015/85
λ1: 68/015
g.
n = 39
λ1-λ2: 015/86
λ1: 70/020
h.
n = 39
λ1-λ2: 013/90
λ1: 70/013
i.
n = 24
λ1-λ2: 174/82
λ1: 80/010

foliation. These intersections are NE-plunging sub-parallel to the hinge lines of the crenulations and folds of compositional layers, and to the mineral lineations.

*4.3.2. Microstructures*

Mineral textures are described based on examination of pairs of thin sections oriented according to rock fabrics (Fig. 7), viz. perpendicular to foliation, and parallel and perpendicular to the mineral elongation lineations. Some sections were cut parallel to foliation. In all sections, the dominant microstructure of non-anatectic rocks in 'straight' belts is a penetrative and continuous mica and quartz-ribbon foliation and a bladed mica lineation (Fig. 7). Both foliation and lineation are readily observed at outcrops of middle amphibolite facies and higher grades (Fig. 7a and b). In foliation-normal thin sections, foliation is domainal (centimeter and millimeter scale Q and P domains), similar to observation at outcrop. The grain size is generally smaller within the P domains (0.1–0.3 mm; Fig. 7), and quartz in both domains shows an apparent weakly preferred *c*-axis fabric (Solar and Brown, 1999). Mica laths that define the foliation are elongated with a strongly preferred orientation defining a mineral elongation lineation that penetrates the rock (Fig. 7). Mica grain shape is strongly bladed, and is determined to be 41:3:1 using the inverse SURFOR wheel method of Panozzo (1987) on the two-dimensional surfaces of the thin sections shown in Fig. 7c and d (Solar, 1999). The mineral elongation lineation is moderately NE-plunging, similar in orientation to the intersection lineation generated by the spaced biotite foliation and the dominant mica foliation, and meter scale fold hinge lines.

The matrix minerals surround porphyroblasts of biotite, garnet, staurolite and andalusite to form both symmetric and less-commonly asymmetric strain shadow tails of quartz and mica aggregates (Solar and Brown, 1999). Asymmetric tails are longest in lineation-parallel views in an orientation parallel to the foliation and lineation in the rock (aspect ratio ~3.5–5; e.g. Fig. 6f). Strain shadow tails around porphyroblasts are also observed in the lineation-perpendicular sections, but with lower aspect ratios (1.5–2.5). Contacts between Q and P domains are deflected around porphyroblasts of staurolite where they occur at or near the contacts (e.g. Fig. 7c; Solar, 1999).

Some observed porphyroblast inclusion trails ($S_i$) are parallel to matrix foliation ($S_e$), but most are discordant. Textural zones commonly are present within garnet and staurolite, defined by the change in orientation of inclusion trails from core to rim. Fig. 8 summarizes rakes between $S_i$ and $S_e$ as measured in lineation-parallel thin sections from 'straight' belt rocks. The results show that $S_i$ rake is consistent in direction in any one thin-section, either up- or down-plunge of the lineation, but varies up to 80° (Fig. 8i).

*4.3.3. Interpretation*

Structural data collected from 'straight' belt rocks at all grades of metamorphism, including migmatite, show a consistency in orientation of all structural elements, which suggests nearly complete transposition of compositional layers into parallelism with the tectonic fabric as defined by the matrix minerals. The exception to this is the locally developed small-scale en echelon structures (Fig. 6), which we interpret to be developed late during the deformation because they crosscut mineral fabrics. Foliation transects meter-scale folds of compositional layers that may mimic the regional-scale folds of the stratigraphic succession (Fig. 4, see section A–A′). The consistency of orientation of both foliation and lineation across the strike of 'straight' belts suggests that the foliation is sub-parallel to the $\lambda_1$–$\lambda_2$ plane, and the lineation is sub-parallel to the direction of maximum principal finite stretch ($\lambda_1$).

Although asymmetric structures record apparently different stages of the progressive deformation (biotite 'fish' and strain shadow tails around porphyroblasts, and en echelon structures), they suggest consistent kinematics. Ramp stacking of compositional layers, as seen in pavement outcrop, shows right-lateral offset (Fig. 6a). Quartz-filled en echelon tension gashes are left-stepping while, in the same outcrop, quartz-filled en echelon shear fractures are right-stepping and 'S' shaped, all suggesting right-lateral sense of shear and layer-parallel offsetting (Fig. 6e). Similarly, in pavement outcrop, left-stepping en echelon ptygmatic folds of granite-filled tension gashes (Fig. 6c) coexist with right-stepping granite-filled shear fractures (Fig. 6d) suggesting right-lateral displacement along the layers. The ptygmatic folds are formed by dextral shear where initially planar veins were folded within the shortening field. In contrast, the coexisting right-stepping granite-filled shear fractures formed initially by shear faulting of the foliation within the domain of lengthening of the same strain ellipsoid. The kinematics are consistent with those determined on steeply oriented surfaces that show SE-side-up displacement. Strain shadow tails around porphyroblasts are elongated within the foliation in the direction of the lineation (Figs. 6f and 7) indicating that displacement was along the steeply dipping foliation, in the direction of the lineation. The asymmetry of these tails is consistent with dextral–SE-side-up oblique kinematics. In outcrops eroded sub-parallel to mineral lineation and in lineation-parallel thin sections,

Fig. 8. Rose diagrams of $S_i$–$S_e$ rakes measured in thin sections cut perpendicular to foliation and parallel to mineral elongation lineation ($\lambda_1$–$\lambda_3$ plane), from rocks in the central 'straight' belt collected at locations across strike (locations (a)–(i) in Fig. 4). Data on diagrams (d)–(h) are from different samples at the same locality along a traverse of ~30 m across strike. The variation in $S_i$–$S_e$ rake in each diagram summarizes data from all porphyroblasts in each thin section. 'n' is the number of measurements. The vertical arrow on each diagram shows both the intersection of the foliation with the diagram, and the plunge direction of the lineation defined by the same minerals.

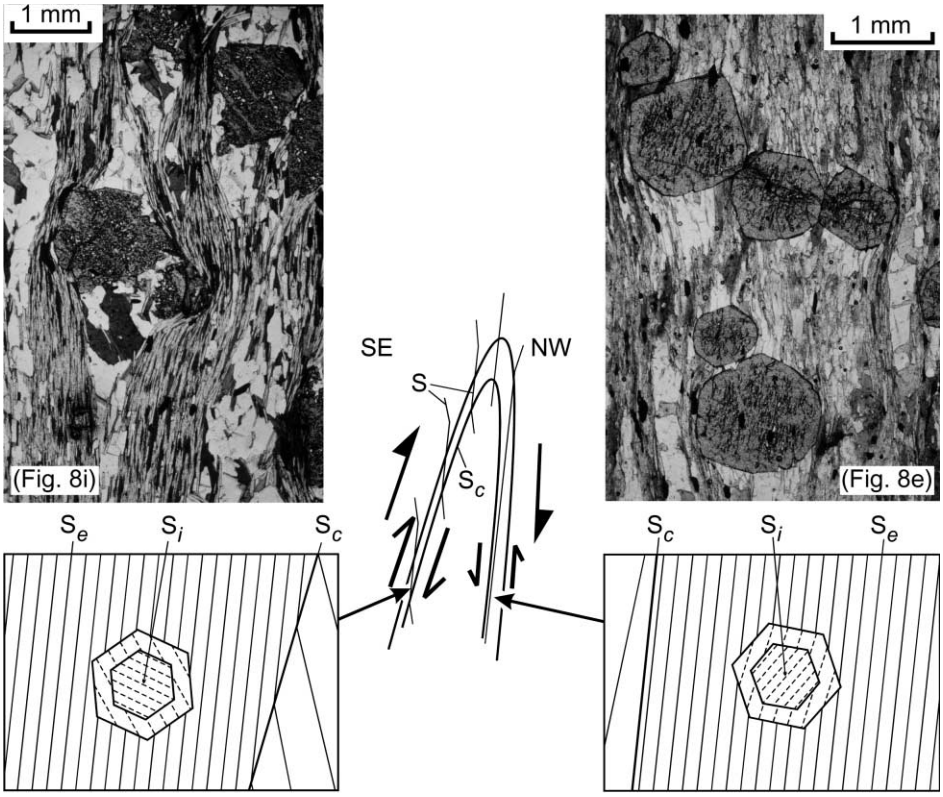


Fig. 9. Interpretation of $S_i$–$S_e$ rake data shown in Fig. 8. Photomicrographs correspond to Fig. 8i and e, respectively, and are oriented parallel to lineation and perpendicular to foliation. The diagram at the center is a sketch of a folded pelite layer that has intersecting foliation that is refracted across the contacts with psammite layers ($S_c$). View of the fold is along the lineation and normal to the foliation in the rock (plane is NE-dipping; parallel to thin sections used for data collection in Fig. 8) to illustrate the interpretation of the obliquity of $S_i$ with respect to $S_e$, as seen in individual porphyroblasts. The sketches at the bottom are close-up views to show the microstructural relations between the external foliation ($S_e$) and the foliation included within the porphyroblasts ($S_i$).

biotite 'fish' are observed 'swimming' up plunge of the lineation to show the same kinematics (Solar and Brown, 1999). The consistent kinematics among different asymmetric structures suggests overall dextral–SE-side-up displacement.

The obliquity between inclusion trails ($S_i$) and matrix foliation ($S_e$), as measured in lineation-parallel thin sections (e.g. Fig. 7c; data in Fig. 8), suggests porphyroblast nucleation and growth occurred before final recrystallization of the matrix minerals (Solar and Brown, 1999). Porphyroblasts grew over the contemporary foliation, and either rotated relative to the foliation, or matrix foliation was reoriented as compositional layers were rotated and flattened during folding. In the latter case, porphyroblasts did not rotate (significantly) relative to contacts between compositional layers (Solar and Brown, 1999). Textural zones within porphyroblasts with a successively smaller rake between $S_i$ and $S_e$ suggest progressive rotation of foliation relative to the porphyroblasts during punctuated porphyroblast growth. Thus, porphyroblast growth was syn- or inter-kinematic in these rocks. Furthermore, the observation that the sense of pitch of $S_i$ is consistent within individual thin sections (Fig. 8), and this pitch alternates in direction across strike of the 'straight' belts, led Solar and Brown (1999) to propose that variations in $S_i$–$S_e$ rake reflect nucleation and growth of porphyroblasts during progressive regional fold tightening of the stratigraphic succession, as shown in Fig. 9. As folds tightened, foliation recrystallized progressively while rotating into a new orientation. Punctuated growth of minerals over this evolving fabric at different stages is recorded by the zonal pattern in porphyroblasts. Variation in $S_i$–$S_e$ rake from porphyroblast to porphyroblast within any one thin section (Fig. 8) suggests nucleation and growth of individual porphyroblasts was diachronous and heterogeneous at the scale of a thin section.

If the mineral fabrics in unmigmatized rocks define the state of finite strain, the ellipsoid defined by grain shapes has an oblate to plane-strain shape ($k \leqslant 1$ on a Flinn plot). This shape is consistent with the similarity in orientation between compositional layers and the foliation across the zone. In migmatite, however, the mineral fabrics define a triaxial to uniaxial oblate ellipsoid ($0 \leqslant k \leqslant 1$). Nonetheless, all rocks within 'straight' belts have fabrics that define oblate shapes. We infer from this that 'straight' belts are zones of $S > L$ tectonite where rocks accommodated apparent flattening-to-plane strain, and we refer to 'straight' belts as "zones of apparent flattening." The general parallelism of compositional layers and tectonic fabric suggests high strain. Consistent with this interpretation, the steeply-dipping, and sub-parallel contacts between compositional layers,

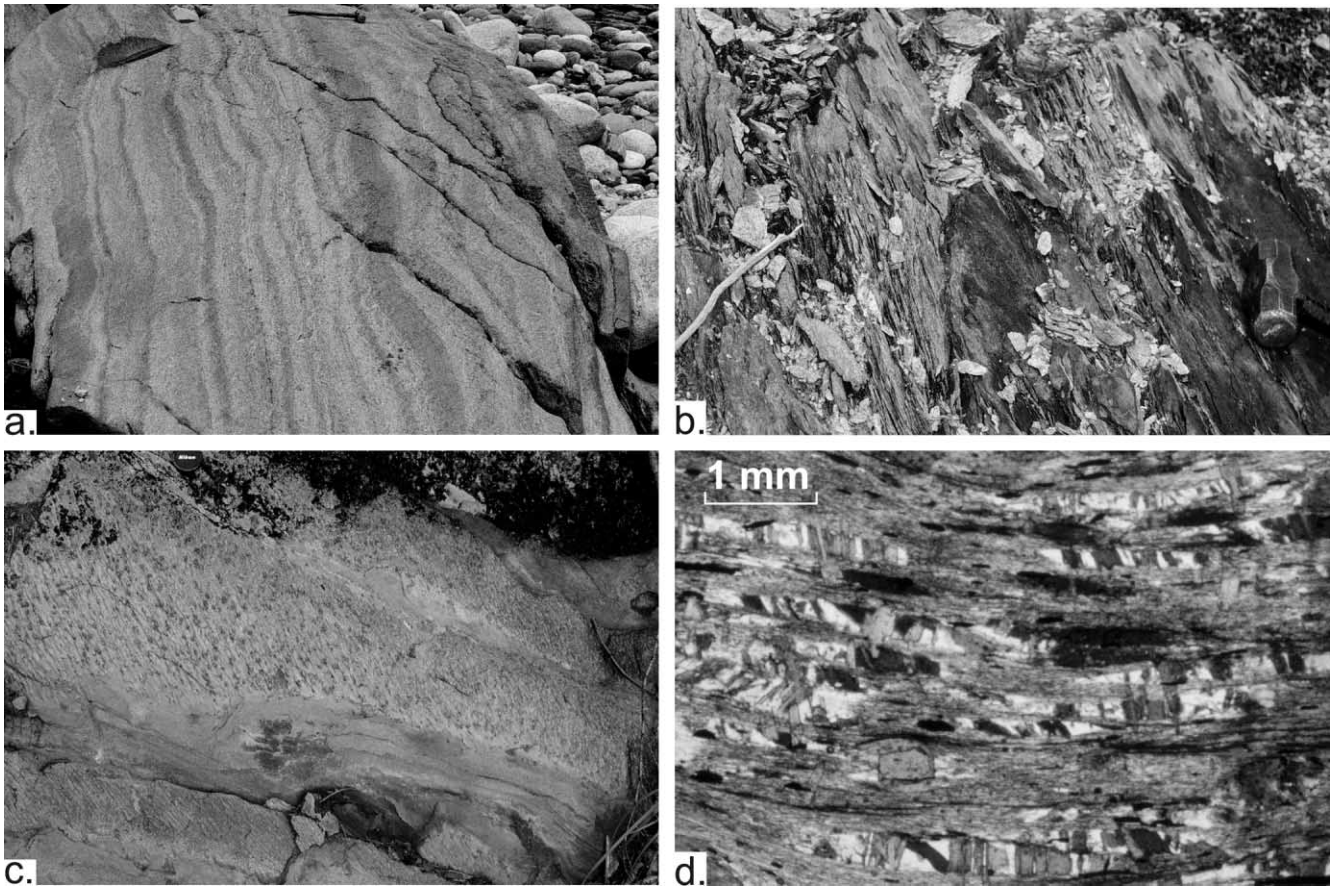


Fig. 10. Structure of rocks in the intervening zones between the 'straight' belts. All examples are from the Rangeley Formation in the intervening zone between the western and central 'straight' belts (compare Figs. 1 and 2). (a) Pavement outcrop in the Swift River, north of Byron Maine displays color banding that illustrates the compositional layers (pelite layers are darker). The layers are deformed into open asymmetric folds. The field of view is to the NE, down-plunge of the mineral elongation lineation in the rock. (b) Photograph oblique to the NE-plunging mineral elongation lineation (NE is to the right), Swift River, N of Byron, Maine. Rocks in the intervening zones that have reached middle amphibolite facies typically weather into rod- or blade-shaped fragments, the long axes of which are parallel to the mineral elongation lineation. (c) Photograph of a SE-dipping surface that shows compositional layers with tectonic fabric in the pelite layers only (NE is to the right), tributary of Swift River, N of Byron, Maine. The field of view is subparallel to the trend of the lineation, defined primarily by rods of quartz aggregates. In this rock there is a weak foliation defined by the coplanar arrangement of the rods. (d) Photomicrograph taken from a thin section cut parallel to the penetrative lineation and perpendicular to the weakly-defined foliation in the rock shown in (a). This microstructure is typical of rocks in the intervening zones. 'Pullaparts' are defined by disaggregated books of biotite (stretched along the bladed muscovite and quartz aggregate-rod lineation).

and the map pattern of the stratigraphic succession together define tight, kilometer-scale folds (Fig. 4, section A–A′; see also Fig. 2, stereograms), consistent with folding in response to finite flattening deformation.

### *4.4. Intervening zones*

#### *4.4.1. Mesostructures*

In contrast to 'straight' belts, rocks in the intervening zones are typified by a variable attitude of compositional layers. Although rock types are similar to those in the adjacent 'straight' belts, the layers in rocks of the intervening zones are less pronounced because contacts between decimeter- and centimeter-scale psammite and pelite layers are not sharp and are gradational over ~1 cm (Fig. 10a–c). No millimeter-scale relict sedimentary structures are observed, except in rocks at lower metamorphic grade, and determination of stratigraphic way up is difficult; recrystallization has erased millimeter-scale bedding, particularly in the pelite layers. The lack of cross-stratification in psammite layers, in contrast with 'straight' belt rocks, may reflect differences in the stratigraphic succession across structural boundaries; e.g. the contact between the Rangeley and Perry Mountain formations is within a structural transition zone (compare Figs. 1 and 2). Also, in contrast with rocks of the 'straight' belts, there is no discernable centimeter scale mineral segregation fabric in the pelite layers (Figs. 10c and 11).

Compositional layers in the intervening zone rocks are meter- to centimeter-scale, and, in contrast to the local meter-scale fold domains found in 'straight' belt rocks, define penetrative meter-scale open folds. Hinge lines of these open folds are moderately NE-plunging (see Fig. 10a). On stereograms, poles to contacts between compositional layers define a girdle distribution that reflects

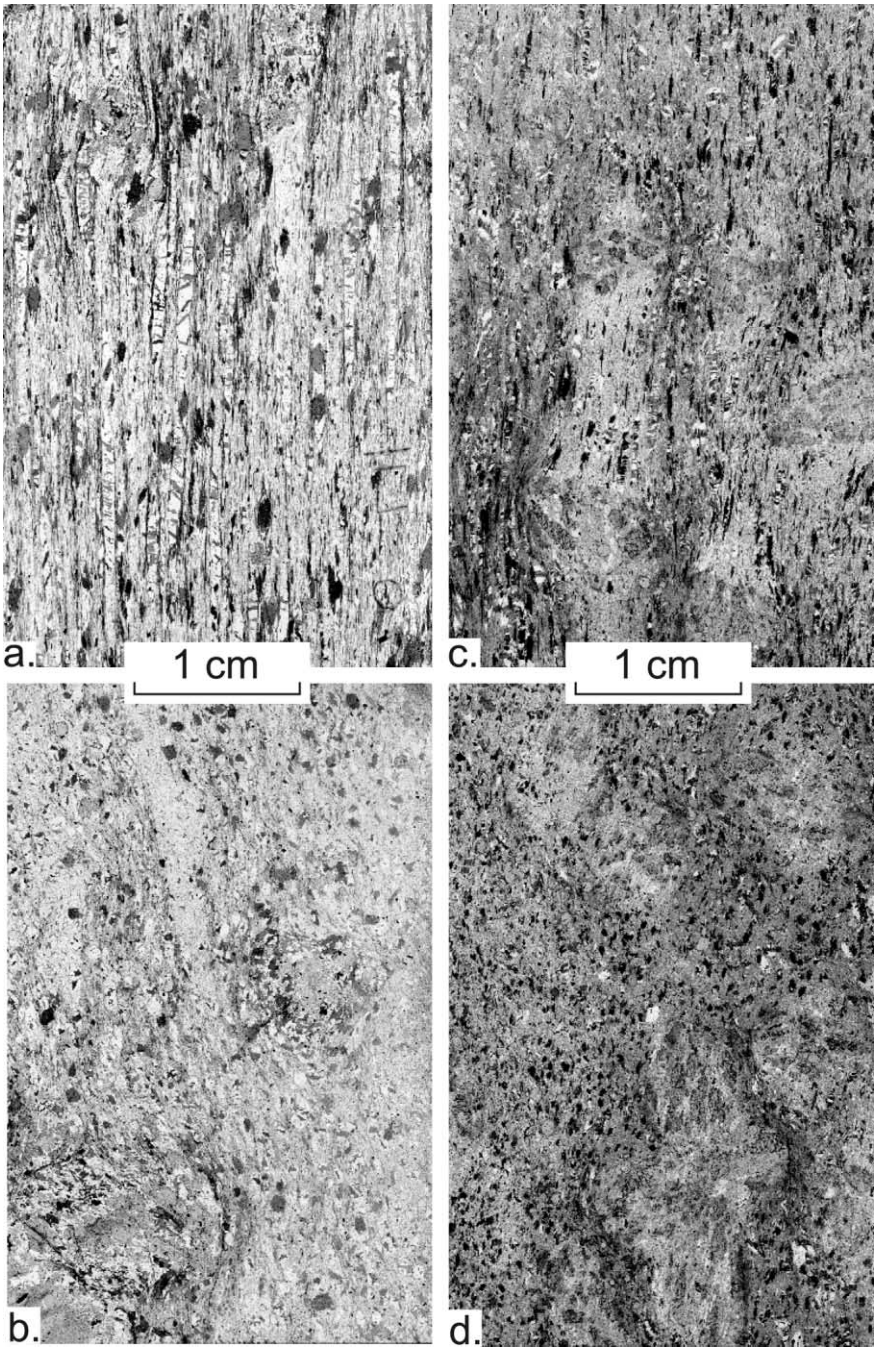


Fig. 11. Microstructural relations in rocks in the intervening zones. This figure shows transmitted light photomicrographs of two pairs of thin sections (a and b are from the rock shown in Fig. 10a and d). Each thin section is cut parallel to lineation (a and c) and perpendicular to lineation (b and d). There is no mineral segregation fabric in any view, in contrast with 'straight' belt rocks (see Fig. 7). Comparison of lineation-parallel and lineation-perpendicular views for both examples shows the penetrative nature of the linear fabric, where grain shapes are conspicuously longer in the lineation-parallel view. The lineation-perpendicular views show this linear fabric in down-plunge view. In (b) and (d), there is a lack of strain shadow tails around porphyroblasts of garnet and biotite, in comparison with (a) and (c), where strain shadow tails are conspicuous. Biotite in (b) and (d) are 'pull-aparts' in down-plunge view. Quartz in (b) and (d) either is in the interboudin partitions within 'pull-aparts', or is part of quartz aggregate rods.

kilometer-scale moderately NE-plunging folds of the stratigraphic succession (Figs. 2 and 3). Where folds of compositional layers are gentle, fold limbs dip moderately between NW and E at all scales. At map-scale, these folds are outlined by the pattern made by the stratigraphic units (Fig. 4, see section A–A′). Hinge zones of folds are rounded to blunt with no discernable axial fabric. In contrast, within 'straight' belts, quartz veins are found in association with folds rarely, and en echelon vein structures have not been observed within or across layers. Boudinage is observed where psammite layers are much thicker than surrounding centimeter-scale interlayered psammite-pelite. Interboudin

partitions are infilled with quartz, and commonly the ductility contrast between layers resulted in the formation of 'fish-mouth' boudinage. Mineral lineations (discussed in the next section) are penetrative and transect folds defined by compositional layers. Mineral fabrics are not parallel to fold hinge lines in outcrop; the hinge lines plunge NE, but more shallowly than the mineral lineations. However, both types of lineations are sub-parallel to each other on a regional basis (see Fig. 2, stereograms).

Structures in pelite layers typically have a penetrative, moderately to steeply N- to NE-plunging mineral elongation lineation, defined by bladed muscovite and rod-shaped aggregates of quartz (Fig. 10b). Psammite layers typically show weak grain-shape fabrics only, which are difficult to recognize at outcrop (Fig. 10c). Foliation is weakly defined, where mica lineations form crude planes in the rock, and shows a large variation in orientation. Poles to both foliation and compositional layers define similar girdles (see stereograms, Fig. 2). In contrast to the layers, foliation is not folded, and instead is fanned about a moderately NE-plunging rotation axis oriented sub-parallel to the mineral elongation lineation, and to the regional fold axis. Fabrics in pelites wrap around porphyroblasts of garnet and staurolite as symmetric tails, giving the rock fabric a crenulated appearance, with the crenulation axes plunging parallel to the lineation (Fig. 10c). This is an artifact of the fabric wrapping the porphyroblasts along the lineation only, describing double-conical strain shadow tails.

Inhomogeneous migmatites in the northern part of the TAD, within the intervening zones, are diatexites that show a penetrative linear structure and a weak planar structure (Solar, 1999). Leucosomes in diatexites are rod-like and meter- to decimeter-scale and granite bodies within the diatexites are cylindrical, both with the axial dimension moderately to steeply NE-plunging. This type of migmatite occurs within intervening zones only, and the granite bodies are concordant to discordant with respect to the linear structure of the host rock (Brown and Solar, 1999).

#### 4.4.2. Microstructures

The dominant microstructure in the intervening zones is a penetrative bladed mica and quartz-rod lineation with common biotite–quartz 'pull-aparts', all of which are readily detectable in outcrops of middle amphibolite facies rocks and above, especially within the Rangeley Formation (Fig. 10). Foliation is weak, but bladed muscovite, which shows a strong preferred orientation, and biotite 'pull-aparts' define a continuous linear fabric (Fig. 11). No Q and P domainal fabric is developed, in contrast to rocks of the 'straight' belts. Matrix mineral grain sizes are generally within the range 0.1–0.3 mm, and surround porphyroblasts of garnet (millimeter scale) and staurolite (centimeter scale). Inclusions in porphyroblasts do not show a preferred orientation in contrast to porphyroblasts in 'straight' belts, except in rocks within the structural transition zones between the 'straight' belts and the intervening zones. If strain shadow tails are present, they are seen in lineation-parallel views only (e.g. Figs. 10d and 11; see also Solar and Brown, 1999) and they are typically symmetrical about the porphyroblast and elongate parallel to lineation, as seen in outcrop (e.g. Fig. 10c).

#### 4.4.3. Interpretation and summary

In rocks of the intervening zones, the compositional layers are not rotated into parallelism with the tectonic fabric, but there is a consistency in orientation of all linear structures. This suggests that these rocks exhibit a different state of finite strain in comparison with rocks in the 'straight' belts. The variable orientation and weak definition of the foliation in these rocks suggests that it did not form parallel to the $\lambda_1$–$\lambda_2$ principal plane, or that this plane has a variable orientation across the intervening zones; however, consistency in orientation of the lineations across the regional strike suggests that they are formed parallel to the maximum principal finite stretch ($\lambda_1$).

Structures in rocks of the intervening zones are symmetrical along the lineation (e.g. strain shadow tails), which implies dominantly coaxial deformation, with a principal finite stretch along the lineation. In outcrops oriented sub-parallel to mineral lineation, and in lineation-parallel thin sections, biotite–quartz 'pull-aparts' are interpreted to be a mineral stretching lineation where biotite books were extended along the direction defined by the length of the muscovite blades, and quartz precipitated between the separated plates. The matrix fabric wraps around the porphyroblasts suggesting that nucleation and growth of porphyroblasts occurred before final recrystallization of the matrix minerals (Solar and Brown, 1999), similar to rocks in the 'straight' belts.

The deformation in intervening zone rocks is defined similarly by structures in both non-migmatitic and migmatitic rocks. If the mineral fabrics in non-migmatitic rocks define the finite strain ellipsoid, then the ellipsoid is a prolate shape ($k \gg 1$), consistent with the well-developed mineral elongation lineation, and the poorly developed foliation, which is not parallel to compositional layers. This is consistent with the similar, but non-parallel attitudes of mineral lineations and compositional-layer fold hinge lines (NE-plunging). The mineral fabrics transect folds, and are interpreted to have formed during the folding due to oblique shear of transposing fold limbs in the direction of the lineation (the maximum principal finite stretch). Similarly, mineral fabrics in migmatite suggest a strongly prolate grain-shape ellipsoid. In both types of rock, the fabric shows apparent constrictional strain. We infer from this that intervening zones are zones of $L \gg S$ tectonite, and we refer to intervening zones as "zones of apparent constriction." Furthermore, the discordance between the orientation of compositional layers and foliation, where present, suggests that the deformation is qualitatively lower than in the 'straight' belts, although the strain magnitude has not been determined quantitatively. In agreement with this

interpretation, at regional scale, the shallowly dipping, and variably oriented contacts between compositional layers, and the map pattern of the stratigraphic succession together define open, kilometer-scale anticlines (Fig. 4, section A–A′; see also Fig. 2, stereograms), consistent with extrusion obliquely out of the map plane.

## 5. Discussion

### 5.1. Regional synthesis

Within the CMB shear zone system, different states of deformation are recorded in two types of structural zone that alternate across strike. In 'straight' belts, rocks have generally oblate grain shape fabrics and tight folds of the stratigraphic succession at all scales (see Figs. 2 and 4), while in the intervening zones, rocks have generally prolate grain shape fabrics and open anticlines without intervening synclines at the kilometer scale (see Figs. 2 and 4). Across the region, at similar grades of metamorphism the same minerals define the different mineral fabrics in the two types of structural zone. Concurrently, in the same structural zone, different minerals appropriate to the different metamorphic grades define similarly oriented and similarly shaped fabrics. We infer from these observations that the two types of zone are parts of the same shear zone system, which developed synchronously across the region during prograde metamorphism that accompanied tightening of folds of the stratigraphic succession and partitioning of deformation. In support of this interpretation, where anatexis occurred, two different structural types of migmatite were formed that correspond to particular structural zones, viz, stromatic migmatite is found in 'straight' belts and inhomogeneous migmatite is found in intervening zones. This suggests that the CMB shear zone system was established before the onset of melting, and that melt flow through the shear zone system was syntectonic.

Taken together, the features we describe suggest that the CMB shear zone system developed during a single progressive deformation within a geologically short period ca. 400 Ma, as suggested by the U–Pb age data of Smith and Barreiro (1990) and Solar et al. (1998). The contrasting patterns of deformation across the region, however, cannot reflect simply the variations in physical properties within and between units of the CMB stratigraphic succession. This is implied by the observation that formation boundaries are transected by boundaries between structural zones (compare Figs. 1 and 2).

### 5.2. Synchronously developed, contrasting states of finite strain during deformation partitioning

Theoretical modeling of deformation paths during transpression suggests that the concept of a steady state deformation path is not appropriate, because it is unreasonable to assume that simple and pure shear strain rates are constant over the history of deformation at any scale (Jiang, 1994; Fossen and Tikoff, 1997; Jiang and Williams, 1999). As $P$–$T$ conditions change during progressive deformation, so must the deformation mechanisms (Knipe, 1989), and non-steady state deformation is expected. Rheological heterogeneities, whether primary or secondary, are dynamic; they will cause heterogeneous partitioning of vorticity and non-coaxiality throughout deforming rocks (Jiang, 1994; Jiang and Williams, 1999). Therefore, the accommodation of deformation is non-steady state during the evolution of transpressive structures. Progressive change in the combination of simple and pure shear end members of the flow is controlled by the evolving rheology. One way of potentially modeling such non-steady state deformation is using the minimum strain path boundary condition of Fossen and Tikoff (1997), in which strain or offset is specified and accommodated internally to the regional structure. It is this internal accommodation that induces heterogeneous deformation so that strain compatibility is maintained at all scales, which may be manifest as discrete structural domains as a consequence of the non-coaxial deformation (Passchier, 1990; Fossen and Tikoff, 1993, 1997; Tikoff and Fossen, 1993). The minimum strain path concept is overly simplistic, however, because there may be as many different minimum strain paths as there are kinematic parameters, and rocks do not deform to achieve arbitrarily specified parameters (Jiang, 1998).

Kinematic partitioning of flow within the CMB occurred early during the accommodation of strain, as folds began to develop in an initially sub-horizontal stratigraphic sequence whose planar anisotropy was sub-parallel to the $\sigma_1$–$\sigma_2$ plane of the far field stress. Once the layers were tilted, the rheological differences between compositional layers and stratigraphic units, and the spacing of slip surfaces, may have become important (Erickson, 1996). As the folds tightened during shortening of the orogen, accommodated by flattening in the 'straight' belts and extrusion of the intervening zones, melting occurred at deep levels in the thickening stratigraphic sequence. The presence of melt lowers the differential stress that can be supported and facilitates reverse (hanging wall up to the south west) displacement due to high fluid pressure (e.g. Sibson, 1985; Brown and Solar, 1998a). Magma migration became important, and melt was drained from a low strength partially molten layer upward through the melt-flow network represented by the CMB shear zone system. Thus, part of the deformation in the deep levels of the system was accommodated by volume loss due to transport of melt to shallow levels in the system.

A model of serial thrusting is used to explain the complex deformation history of the CMB shear zone system. This model is illustrated in two dimensions in Fig. 12. The early part of the deformation history was dominated by thrusting along listric ramps that transected the stratigraphic units. The alternating zones of contrasting states of finite strain were produced because of instabilities in the flow regime

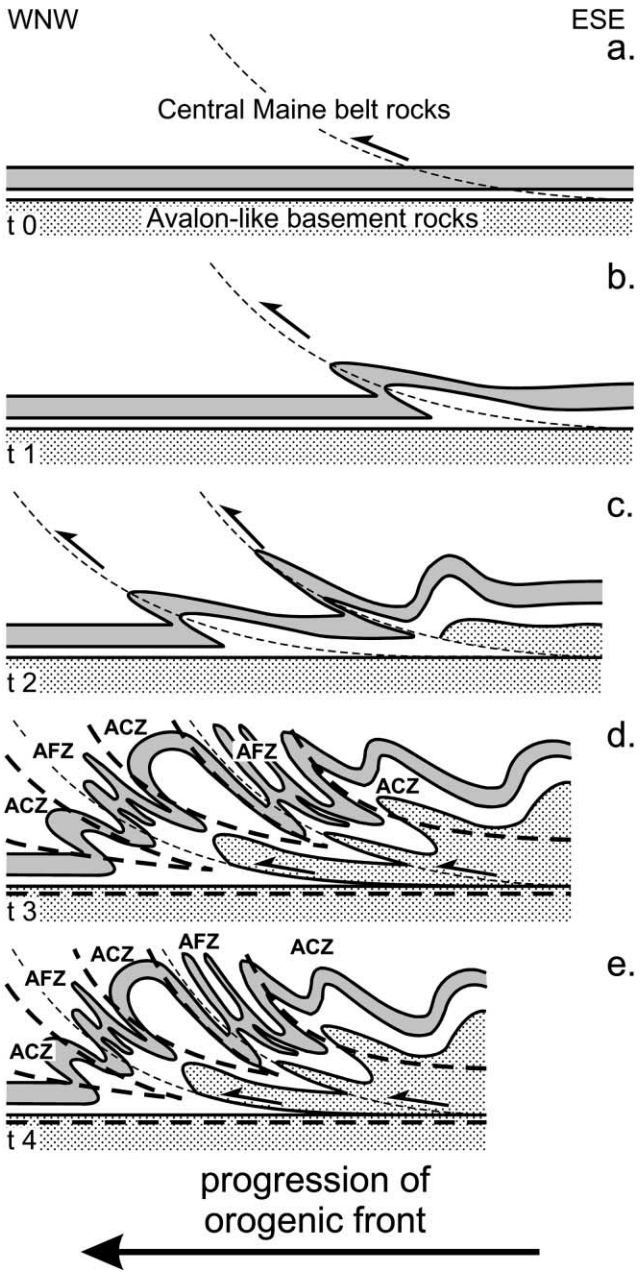


that developed at these ramps. Deformation at the ramps involved enhanced simple shear flow in comparison with the zones inbetween. Ramping likely progressed inboard (SE to NW) and from top to bottom, according to models of thrust system evolution (e.g. Boyer and Elliott, 1982, and references therein). Although the geometry of ramps in the deep crust remains controversial (Ramsay et al., 1988), we assume that ramps were spaced evenly across the CMB (Fig. 12c and d), as suggested by the experimental work of Goff (reported in Erickson, 1996). As the system evolved, the periodicity of fold instabilities, particularly the thrust ramp anticlines, controlled the spacing of zones where simple shear flow was enhanced. The processes of strain softening in the zones of simple shear flow enabled them to accommodate more flattening (biaxial) strain, as recorded by the oblate grain shape fabrics that define the 'straight' belts. These oblate fabrics formed progressively during fold tightening. Shortening accommodated by the flattening in the thrust zones produced strain incompatibilities, and rocks within the intervening zones between the thrust ramp anticlines were extruded to maintain strain compatibility (e.g. Robin and Cruden, 1994). As the system evolved, the initial 'ramp-flat' geometry (e.g. Fig. 12a) became modified progressively by tightening of folds (e.g. Fig. 12c–e). In the intervening zones, although prolate fabrics were developed, the strain may have been plane (Freeman, 1985). Strain softening in the ramp zones may have been concomitant with strain hardening in the intervening zones, enhancing rheological contrasts between the two zones. This contrast would stabilize the evolving fabrics in the alternating zones. The steep dips of ramp zones in Fig. 12e, and of 'straight' belts in Fig. 4 (structure sections) are interpreted to reflect late increased flattening in those zones that steepened them from more moderate dip angles (e.g. Fig. 12b–d).

The two-dimensional model shown in Fig. 12 explains the alternating pattern of structural zones across strike, but does not explain explicitly why prolate grain-shape fabrics developed in rocks between the thrust ramps, except for the tendency of multiparticulate fabrics to be prolate (Freeman, 1985). Other factors may contribute to the development of apparent constriction fabrics. Models of transpressional and transtensional structural development predict that constrictional strain should be limited to transtensional shear zones (e.g. Dewey et al., 1999), unless there is a volume change (e.g. Fossen and Tikoff, 1993). Few cases of prolate fabrics are documented in belts formed by transpression, and these are interpreted either as local instabilities (Hudleston et al.,

Fig. 12. A set of schematic model sections to show the proposed evolution of the CMB shear zone system. The shaded fields are the same unit at $t_0$–$t_4$, and represent the folds of the Rangeley stratigraphic sequence (cf. Fig. 4, section A–A′) during the development of the structure. At time 0 (a), the Rangeley stratigraphic sequence lay undeformed above the Avalon-like basement rocks (stippled field). As the crust shortened, and was contracted inboard [$t_1$, (b)], the sequence began to buckle asymmetrically to form a ramp-like anticline in the middle crust. The CMB–basement contact is interpreted to have been the zone of décollement for the detachment. These folds correspond to contemporary thrust ramps in the shallower crust. As the system evolved during progressive contraction, deformation was localized within the volume of folded rocks, and the folds were tightened which likely caused progressive strain hardening of these rocks. As a result of the strain hardening, a splay formed inboard to produce a second set of folds [$t_2$ (c)]. As the system evolved further, shortening was accommodated more easily within the volumes of folded rocks to form zones of apparent flattening strain (AFZs) separated by intervening blocks (zones of apparent constrictional strain; ACZs). The alternation between zones corresponds to the areas of tight and open folds, respectively [(d) and (e)]. Increased flattening in ramp zones steepened their dips [$t_2$ to $t_4$, (c) to (e); cf. structure sections in Fig. 4]. The thick dashed lines in (d) and (e) are boundaries between the two types of structural zone (cf. Fig. 4). Although not shown (for simplicity), translation along the shear surfaces within the zones of flattening (dashed curves) likely produced thrusts that disrupted fold limbs (section A–A′, Fig. 4).

1988), or as having formed in belts where the crust was extended laterally along the shear zone boundaries (Dias and Ribeiro, 1994). The three-dimensional geometry of the CMB shear zone system is apparent from the maps and structure sections of Figs. 2 and 4. 'Straight' belts are arcuate (southeast) to straight (northwest) and through-going in plan view, and downward-converging in cross-section view. In contrast, intervening zones are lens-shaped at deeper structural levels in the southeast, around the Phillips pluton and encompassing the TAD and WAD, but wedge-shaped at shallower structural levels in the northwest around the Redington, Sugarloaf and northern lobe of the Lexington plutons. These observations suggest that the geometry of the thrust ramps of Fig. 12 curves into and out of the structure sections at deeper levels in the crust, represented by the southeast side of the study area, i.e. the geometry is truly listric in three-dimensions, but straightens with decreasing depth in the crust. Although deformation in this geometry involves divergent flow in the shear zone system as a whole, extrusion of the intervening zones is inferred to involve essentially outward flow as the shear zone system lengthens. Extrusion by outward flow should stabilize the fabric elements, particularly the correspondence in orientation between the axis of maximum finite elongation and the direction of maximum extensional flow (Passchier, 1997; Teyssier and Tikoff, 1999). This interpretation is supported by the limited variation in lineation plunge both along and across the CMB, with a larger variation in intervening zones (Fig. 2), consistent with the inference that it records the flow direction.

Fabrics in the zones of apparent constriction may not reflect the bulk flow field directly (e.g. Freeman, 1985), which may be close to plane strain, but rather record evidence of a relative increase in volume compared with the zones of apparent flattening (Brown and Solar, 1998a), suggesting that some component of constriction may be real. In migmatite in intervening zones, syntectonically formed linear leucosomes and meter-scale granite bodies with long dimensions subparallel to the mineral lineation in the matrix, and plutons in the region with conical roots inside the intervening zones, suggest that magma preferentially accumulated in these zones (Brown and Solar, 1999). Thus subsolidus and suprasolidus rocks in the intervening zones record close to uniaxial deformation.

The two contrasting types of deformation zone are not separated by discrete boundaries, from which evidence we infer that the two types of grain-shape fabrics did not develop exclusively in the two structural zones. On the contrary, observations of fabrics at the transition zones between 'straight' belts and intervening zones show a progression where oblate fabrics diminish along a traverse across strike into intervening zone rocks. The transition zones are interpreted to record the encroachment of the zones of flattening strain on the zones of constriction as material is transferred concomitantly from the zones of flattening to the intervening zones to maintain a uniaxial deformation during volume increase. This is supported by the apparent volume increase recorded by the precipitation of quartz between separated biotite plates in the biotite–quartz pull-aparts, and the location of pluton roots in the intervening zones (Figs. 2 and 4).

These observations are consistent with an alternation in these two types of zone of the three-dimensional strain facies as developed by Tikoff and Fossen (1999). These different strain facies imply different types of thinning and thickening transpressional shear zones. Comparing fabrics in the CMB to the strain facies of Tikoff and Fossen (1999), the zones of apparent flattening correspond with oblique foliation/oblique lineation (strain facies 4), while the zones of apparent constriction correspond with transverse foliation/oblique lineation (strain facies 5). This correlation implies a thickening deformation zone. Alternatively, the more consistent orientation of the lineation in the zones of apparent flattening suggests these zones are close to shear-parallel foliation/shear-parallel lineation (strain facies 1), while the increased variability in lineation orientation in the zones of apparent constriction suggests a larger obliquity between the lineation and the shear direction in these zones. This second correlation implies a thinning deformation zone for the zones of apparent flattening and a thickening deformation zone for the zones of apparent constriction. In either correlation, however, the strain facies must be different from zone to zone to maintain a listric three-dimensional geometry of the CMB shear zone system. A caveat to both correlations is the dependence of the model on a steady state flow regime to produce the fabrics associated with the strain facies. However, the model appears to corroborate a difference in deformation history between the two types of structural zone in the CMB shear zone system.

Concentration or localization of displacement in the 'straight' belts is the result of accommodation of apparent flattening in those zones, consistent with models of transpressional zones (e.g. Dewey et al., 1999). This localization implies that the 'straight' belts are also zones of higher displacement and higher strain (the HSZs of Brown and Solar, 1998a,b, 1999; Solar and Brown, 1999) in relation to the intervening zones of apparent constriction, which are zones of lower strain (the LSZs of Brown and Solar, 1998a,b, 1999; Solar and Brown, 1999). The alternating oblate–prolate structural pattern of the CMB is similar in style to that of the Shimanto and Sambagawa metamorphic belts of Japan, respectively, although different in tectonic setting. Oblate fabrics are found in the Shimanto belt, at the continental margin where a more biaxial deformation was accommodated during subduction, while prolate fabrics are found inboard, in the Sambagawa belt, in the tectonic wedge, where a more uniaxial extension was accommodated (Toriumi, 1985; Toriumi and Noda, 1986).

The interpretation that zones of apparent flattening are developed at spaced thrust ramps is consistent with field relations where these zones mark important stratigraphic contacts. Comparing Figs. 1, 2 and 4, the western 'straight'

belt/zone of apparent flattening occurs at the upper BHB–lower CMB contact, which we interpret to be the inboard tectonic 'backstop' to the regional structure. The Silurian stratigraphic sequence is repeated in the eastern part of the study area, beginning at the eastern margin of the central 'straight' belt/zone of apparent flattening, consistent with reverse displacement across that belt. Although we have not mapped to the east of the eastern 'straight' belt/zone of apparent flattening, we suggest that this structure marks another thrust.

## 6. Conclusion

We interpret the CMB shear zone system to have developed as a thrust system during dextral–transpressive deformation in response to Early Devonian (Acadian) oblique convergence. The deformation was partitioned between zones of apparent flattening strain and zones of apparent constrictional strain. This partitioning was a consequence of the serial development and subsequent progressive modification of thrust ramps in the Silurian to Early Devonian stratigraphic succession above the Avalon-like basement. A relative increase in volume in the zones of apparent constrictional strain as the zones of apparent flattening strain encroached on them with progressive accommodation of strain is suggested as a mechanism to maintain the prolate fabrics. The model is consistent with models of transpression zones, where strain is distributed heterogeneously into belts of contrasting finite deformation (Robin and Cruden, 1994), and in which the transpression zone is stretched along strike (Dias and Ribeiro, 1994). Further, our model for the evolution of structures in western Maine (Fig. 12) is consistent with the tectonic model for the Acadian orogeny of Bradley (1998), which primarily uses the crystallization age of plutons to suggest that the Acadian orogenic front migrated inboard during the Devonian.

## Acknowledgements

We acknowledge helpful discussions with many people, including Spike Berry, Bob Marvinney, Bob Moench, Ed Sawyer, Dave Stewart, Cees van Staal and E-an Zen. Thoughtful critical reviews by Haakon Fossen, Dazhi Jiang, Rick Law and an anonymous reviewer, and the editing of Shoufa Lin, helped to clarify the content and interpretations in the paper. We acknowledge partial support of this work from the Department of Geology, University of Maryland, the Geological Society of America Research Grants Program and NSF Grant EAR-9705858.

## References

Boyer, S.E., Elliott, D., 1982. Thrust systems. Bulletin of the American Association of Petroleum Geology 66, 1196–1230.

Bradley, D.C., 1983. Tectonics of the Acadian orogeny in New England and adjacent Canada. Journal of Geology 91, 381–400.

Bradley, D.C., Tucker, R.D., Lux, D.R., Harris, A.G., McGregor, D.C., 1998. Migration of the Acadian orogen and foreland basin across the northern Appalachians. U.S. Geological Survey, Open-File Report 98–770, 79p.

Braun, J., Beaumont, C., 1995. Three-dimensional numerical experiments of strain partitioning at oblique plate boundaries: implication for contrasting tectonic styles in the Southern Coast Ranges, California, and Central South Island, New Zealand. Journal of Geophysical Research 100, 18058–18074.

Brown, M., Rushmer, T., 1997. The role of deformation in the movement of granite melt: views from the laboratory and the field. In: Holness, M.B. (Ed.). Deformation-enhanced Fluid Transport in the Earth's Crust and Mantle. The Mineralogical Society Series 8. Chapman and Hall, London, pp. 111–144.

Brown, M., Solar, G.S., 1998a. Shear zones and melts: positive feedback in orogenic belts. Journal of Structural Geology 20, 217–231.

Brown, M., Solar, G.S., 1998b. Granite ascent and emplacement during contractional deformation in convergent orogens. Journal of Structural Geology 20, 1365–1393.

Brown, M., Solar, G.S., 1999. The mechanism of ascent and emplacement of granite magma during transpression: a syntectonic granite paradigm. Tectonophysics 312, 1–33.

Burg, J.-P., 1999. Ductile structures and instabilities: their implication for Variscan tectonics in the Ardennes. Tectonophysics 309, 1–25.

Chamberlain, C.P., England, P.C., 1985. The Acadian thermal history of the Merrimack Synclinorium in New Hampshire. Journal of Geology 93, 593–602.

Cobbold, P., 1976. Mechanical effects of anisotropy during large finite deformations. Bulletin Société géologique de France 18, 1497–1510.

Cocks, L.R.M., McKerrow, W.S., van Staal, C.R., 1997. The margins of Avalonia. Geological Magazine 134, 627–636.

D'Lemos, R.S., Brown, M., Strachan, R.A., 1992. Granite magma generation, ascent and emplacement within a transpressional orogen. Journal of the Geological Society 149, 487–490.

De Yoreo, J.J., Lux, D.R., Guidotti, C.V., 1991. Thermal modelling in low-pressure/high-temperature metamorphic belts. Tectonophysics 188, 209–238.

Dewey, J.F., Holdsworth, R.E., Strachan, R.A., 1999. Transpression and transtension zones. In: Holdsworth, R.E., Strachan, R.A., Dewey, J.F. (Eds.). Continental Transpressional and Transtensional Tectonics. Geological Society, London, pp. 1–14 Special Publication 135.

Dias, R., Ribeiro, A., 1994. Constriction in a transpressive regime: an example in the Iberian branch of the Ibero–Armorican arc. Journal of Structural Geology 16, 1543–1554.

Elliott, D., 1972. Deformation paths in structural geology. Geological Society of America Bulletin 83, 2621–2638.

Erickson, S.G., 1996. Influence of mechanical stratigraphy on folding vs faulting. Journal of Structural Geology 18, 443–450.

Eusden Jr, J.D., Barreiro, B., 1988. The timing of peak high-grade metamorphism in central-eastern New England. Maritime Sedimentation and Atlantic Geology 24, 241–255.

Eusden Jr, J.D., Garesche, J.M., Johnson, A.H., Maconochie, J.-M., Peters, S.P., O'Brien, J.B., Widmann, B.L., 1996. Stratigraphy and ductile structure of the Presidential Range, New Hampshire: tectonic implications for the Acadian orogeny. Geological Society of America Bulletin 108, 417–436.

Fitch, T.J., 1972. Plate convergence, transcurrent faults, and internal deformation adjacent to southeast Asia and the western Pacific. Journal of Geophysical Research 77, 4432–4460.

Fossen, H., Tikoff, B., 1993. The deformation matrix for simultaneous simple shearing, pure shearing, and volume change, and its application to transpression/transtension tectonics. Journal of Structural Geology 15, 413–422.

Fossen, H., Tikoff, B., 1997. Forward modeling of non-steady state deformations and the 'minimum strain path'. Journal of Structural Geology 19, 987–996.

Freeman, B., 1985. The motion of rigid ellipsoidal particles in slow flows. Tectonophysics 113, 163–183.

Gordon, R.G., 1995. Plate motions, crustal and lithospheric mobility, and paleomagnetism: Prospective view point. Journal of Geophysical Research 100, 24367–24392.

Grocott, J., Brown, M., Dallmeyer, R.D., Taylor, G.K., Treloar, P.J., 1994. Mechanisms of continental growth in extensional arcs: an example from the Andean Plate Boundary Zone. Geology 22, 391–394.

Guidotti, C.V., 1970. The mineralogy and petrology of the transition from lower to upper sillimanite zone in the Oquossoc area, Maine. Journal of Petrology 11, 277–336.

Guidotti, C.V., 1974. Transition from staurolite to sillimanite zone, Rangeley quadrangle, Maine. Geological Society of America Bulletin 85, 475–490.

Guidotti, C.V., 1989. Metamorphism in Maine: an overview. In: Tucker, R.D., Marvinney, R.G. (Eds.). Igneous and Metamorphic Geology, Volume 3: Studies in Maine Geology. Maine Geological Survey, pp. 1–19.

Harland, W.B., 1971. Tectonic transpression in Caledonian Spitsbergen. Geological Magazine 108, 27–42.

Hatch Jr, N.L., Moench, R.H., Lyon, J.B., 1983. Silurian-lower Devonian stratigraphy of eastern and south-central New Hampshire: extensions from western Maine. American Journal of Science 283, 739–761.

Holdaway, M.J., Guidotti, C.V., Novak, J.M., Henry, W.E., 1982. Polymetamorphism in medium- to high-grade pelitic metamorphic rocks, west-central Maine. Geological Society of America Bulletin 93, 572–584.

Holdaway, M.J., Mukhapodhyay, B., Dyar, M.D., Guidotti, C.V., Dutrow, B.L., 1997. Garnet-biotite geothermometry revised: new Margules parameters and a natural specimen data set from Maine. American Mineralogist 82, 582–595.

Hollister, L.S., Crawford, M.L., 1986. Melt-enhanced deformation: a major tectonic process. Geology 14, 558–561.

Hubbard, M.S., West Jr, D.P., Ludman, A., Guidotti, C.V., Lux, D.R., 1995. The Norumbega fault zone, Maine: a mid- to shallow-level crustal section within a transcurrent shear zone. Atlantic Geology 31, 109–116.

Hudleston, P., Schultz-Ela, D., Southwick, D., 1988. Transpression in an Archean greenstone belt, northern Minnesota. Canadian Journal of Earth Science 25, 1060–1068.

Jiang, D., 1994. Vorticity determination, distribution, partitioning and the heterogeneity and non-steadiness of natural deformations. Journal of Structural Geology 16, 121–130.

Jiang, D., 1998. Forward modeling of non-steady-state deformation and the 'minimum strain path': discussion. Journal of Structural Geology 20, 975–977.

Jiang, D., Williams, P.F., 1998. High-strain zones: a unified model. Journal of Structural Geology 20, 1105–1120.

Jiang, D., Williams, P.F., 1999. A fundamental problem with kinematic interpretation of geological structures. Journal of Structural Geology 21, 933–937.

Jones, R.R., Tanner, P.W.G., 1995. Strain partitioning in transpression zones. Journal of Structural Geology 17, 793–802.

Knipe, R.J., 1989. Deformation mechanisms recognition from natural tectonites. Journal of Structural Geology 11, 127–146.

Lin, S., Jiang, D., Williams, P.F., 1998. Transpression (or transtension) zones of triclinic symmetry: natural example and theoretical modelling. In: Holdsworth, R.E., Strachan, R.A., Dewey, J.F. (Eds.). Continental Transpressional and Transtensional Tectonics. Geological Society, London, pp. 41–57 Special Publication 135.

Lister, G.S., Williams, P.F., 1983. The partitioning of deformation in flowing rock masses. Tectonophysics 92, 1–33.

Liu, X., McNally, K.C., Shen, Z.-K., 1995. Evidence for a role of the downgoing slab in earthquake slip partitioning at oblique subduction zones. Journal of Geophysical Research 100, 15351–15372.

Ludman, A., 1998. Evolution of a transcurrent fault system in shallow crustal metasedimentary rocks: the Norumbega fault zone, eastern Maine. Journal of Structural Geology 20, 93–107.

McCaffrey, R., 1992. Oblique plate convergence, slip vectors, and forearc deformation. Journal of Geophysical Research 97, 8905–8915.

Means, W.D., Hobbs, B.E., Lister, G.S., Williams, P.F., 1980. Vorticity and non-coaxiality in progressive deformation. Journal of Structural Geology 2, 371–378.

Moench, R.H., 1969. The Quimby and Greenvale Cove Formations in western Maine. U.S. Geological Survey Professional Paper 1274-L, pp. L1–L17.

Moench, R.H., 1970. Evidence for premetamorphic faulting in the Rangeley quadrangle, western Maine. Guidebook for Field Trips in The Rangeley Lakes – Dead River Region, Western Maine, New England Intercollegiate Geological Conference, 62nd Annual Meeting, pp. D:1–12.

Moench, R.H., 1970b. Premetamorphic down-to-basin faulting, folding, and tectonic dewatering, Rangeley area, western Maine. Geological Society of America Bulletin 81, 1463–1496.

Moench, R.H., 1971. Geologic map of the Rangeley and Phillips quadrangles. Franklin and Oxford Counties, Maine. U.S. Geological Survey Map I-605, scale 1:62,500.

Moench, R.H., Boudette, E.L., 1970. Stratigraphy of the northwest limb of the Merrimack synclinorium in the Kennebago Lake, Rangeley, and Phillips quadrangles, western Maine. Guidebook for Field Trips in the Rangeley Lakes—Dead River Region, Western Maine, New England Intercollegiate Geological Conference, 62nd Annual Meeting, pp. A:1–25.

Moench, R.H., Pankiwskyj, K.A., 1988. Definition, problems, and reinterpretation of early premetamorphic faults in western Maine and northeastern New Hampshire. In: Tucker, R.D., Marvinney, R.G. (Eds.). Studies in Maine Geology, Volume 1: Structure and Stratigraphy. Maine Geological Survey, pp. 35–50.

Moench, R.H., Boone, G.M., Bothner, W.A., Boudette, E.L., Hatch, N.L., Jr., Hussey, A.M., II, Marvinney, R.G., Aleinikoff, J.N., 1995. Geologic map of the Sherbrooke–Lewiston area, Maine, New Hampshire and Vermont, United States and Quebec, Canada. U.S. Geological Survey Map I-1898-D, scale 1:250,000.

Musacchio, G., Mooney, W.D., Luetgert, J.H., 1997. Composition of the crust in the Grenville and Appalachian Provinces of North America inferred from VP/VS ratios. Journal of Geophysical Research 102, 15225–15241.

Osberg, P.H., Moench, R.H., Warner, J., 1968. Stratigraphy of the Merrimack Synclinorium in west-central Maine. In: Zen, E-an, White, W.S., Hadley, J.B. (Eds.). Studies of Appalachian Geology: Northern and Maritime. Interscience Publishers, New York, pp. 241–253.

Panozzo, R., 1987. Two-dimensional strain determination by the inverse SURFOR wheel. Journal of Structural Geology 9, 115–119.

Passchier, C.W., 1990. Reconstruction of deformation and flow parameters from deformed vein sets. Tectonophysics 180, 185–199.

Passchier, C.W., 1997. The fabric attractor. Journal of Structural Geology 19, 113–127.

Passchier, C.W., Trouw, R.A.J., 1996. Microtectonics. Springer-Verlag, Berlin, Heidelberg.

Pavlis, T.L., 1996. Fabric development in syn-tectonic intrusive sheets as a consequence of melt-dominated flow and thermal softening of the crust. Tectonophysics 253, 1–31.

Pressley, R.A., Brown, M., 1999. The Phillips Pluton, Maine, USA: evidence of heterogeneous crustal sources, and implications for granite ascent and emplacement mechanisms in convergent orogens. Lithos 46, 335–366.

Ramsay, J.G., Graham, R.H., 1970. Strain variation in shear belts. Canadian Journal of Earth Sciences 7, 786–813.

Ramsay, J.G., Butler, R.W.H., Coward, M.P., 1988. General discussion. Philosophical Transactions of the Royal Society of London A326, 321–325.

Ratcliffe, N.M., Hames, W.E., Stanley, R.S., 1998. Interpretation of ages of arc magmatism, metamorphism, and collisional tectonics in the Taconian orogen of western New England. American Journal of Science 298, 791–797.

Robin, P.-Y.F., Cruden, A.R., 1994. Strain and vorticity patterns in ideally ductile transpression zones. Journal of Structural Geology 16, 447–467.

Robinson, P., Tucker, R.D., Bradley, D., Berry IV, H.N., Osberg, P.H., 1998. Paleozoic orogens in New England, USA. Geologiska Föreningens i Stockholm Förhandlingar 120, 119–148.

Royden, L., 1996. Coupling and decoupling of crust and mantle in convergent orogens: implication for strain partitioning in the crust. Journal of Geophysical Research 101, 16679–17705.

Rutter, E.H., Brodie, K.H., 1995. Mechanistic interactions between deformation and metamorphism. Geological Journal 30, 227–240.

Rutter, E., Neumann, D., 1995. Experimental deformation of partially molten Westerly granite under fluid-absent conditions, with implications for the extraction of granitic magmas. Journal of Geophysical Research 100 (15), 697–715.

Sawyer, E.W., 1999. Criteria for the recognition of partial melting. Physics and Chemistry of the Earth 24, 269–279.

Sibson, R.H., 1985. A note on fault reactivation. Journal of Structural Geology 7, 751–754.

Smith, H.A., Barreiro, B., 1990. Monazite U–Pb dating of staurolite grade metamorphism in pelitic schists. Contributions to Mineralogy and Petrology 105, 602–615.

Solar, G.S., 1999. Structural and petrological investigations in the Central Maine belt, west-central Maine, with special reference to the migmatites. Ph.D. thesis, University of Maryland.

Solar, G.S., Brown, M., 1999. The classic high-*T*–low-*P* metamorphism of west-central Maine, USA: Is it post-tectonic or syn-tectonic? Evidence from porphyroblast-matrix relations. Canadian Mineralogist 37, 311–333.

Solar, G.S., Pressley, R.A., Brown, M., Tucker, R.D., 1998. Granite ascent in convergent orogenic belts: testing a model. Geology 26, 711–714.

Stewart, D.B., 1989. Crustal processes in Maine. American Mineralogist 74, 698–714.

Stewart, D.B., Wright, B.E., Unger, J.D., Phillips, J.D., Hutchinson, D.R. (principal compilers), 1992. Global geoscience transect 8: Quebec–Maine–Gulf of Maine Transect, southeastern Canada, northeastern United States of America. U.S. Geological Survey Map I-2329.

Swanson, M.T., 1992. Late Acadian–Alleghenian transpressional deformation: evidence from asymmetric boudinage in the Casco Bay area, coastal Maine. Journal of Structural Geology 14, 323–341.

Teyssier, C., Tikoff, B., 1999. Fabric stability in oblique convergence and divergence. Journal of Structural Geology 21, 969–974.

Teyssier, C., Tikoff, B., Markley, M., 1995. Oblique plate motion and continental tectonics. Geology 23, 447–450.

Tikoff, B., Fossen, H., 1993. Simultaneous pure and simple shear: the unifying deformation matrix. Tectonophysics 217, 267–283.

Tikoff, B., Fossen, H., 1999. Three-dimensional reference deformations and strain facies. Journal of Structural Geology 21, 1497–1512.

Tomascak, P.B., Krogstad, E.J., Walker, R.J., 1996. U–Pb monazite geochronology of granitic rocks from Maine: implications for Late Paleozoic tectonics in the northern Appalachians. Journal of Geology 104, 185–195.

Toriumi, M., 1985. Two types of ductile deformation/regional metamorphic belt. Tectonophysics 113, 307–326.

Toriumi, M., Noda, H., 1986. The origin of strain patterns resulting from contemporaneous deformation and metamorphism in the Sambagawa metamorphic belt. Journal of Metamorphic Geology 4, 409–420.

Unger, J.D., Liberty, L.M., Phillips, J.D., Wright, B.E., 1989. Creating a 3-dimensional transect of the earth's crust from craton to ocean basin across the N. Appalachian Orogen. In: Raper, J. (Ed.). 3-Dimensional Applications in Geographical Information Systems. Taylor and Francis, London, pp. 137–148.

van Staal, C.R., de Roo, J.A., 1995. Mid-Paleozoic tectonic evolution of the Appalachian Central Mobile Belt in northern New Brunswick, Canada: collision, extensional collapse and dextral transpression. In: Hibbard, J.P., van Staal, C.R., Cawood, P.A. (Eds.). Current Perspectives in the Appalachian–Caledonian Orogen, pp. 367–389 Geological Association of Canada Special Paper 41.

van, Staal, C.R., Dewey, J.F., MacNiocaill, C., McKerrow, W.S., 1998. The Cambrian–Silurian tectonic evolution of the northern Appalachians and British Caledonides: history of a complex, west and southwest Pacific-type segment of Iapetus. Geological Society Special Publication.

West, D.P., 1999. Timing of displacements along the Norumbega fault system, south-central and south-coastal Maine. In: Ludman, A., West, D.P. (Eds.). Norumbega Fault System of the Northern Appalachians. Geological Society of America Special Paper 331, pp. 167–178.

West Jr, D.P., Hubbard, M.S., 1997. Progressive localization of deformation during exhumation of a major strike-slip shear zone: Norumbega fault zone, south-central Maine. Tectonophysics 273, 185–202.

West Jr, D.P., Guidotti, C.V., Lux, D.R., 1995. Silurian orogenesis in the western Penobscot Bay region, Maine. Canadian Journal of Earth Sciences 32, 1845–1858.

White, S.H., Knipe, R.J., 1978. Transformation- and reaction-enhanced ductility in rocks. Journal of Geological Society 135, 513–516.

Williams, H., 1978. Structural telescoping across the Appalachian orogen and the minimum width of the Iapetus Ocean. In: Strangway, D.W. (Ed.). The Continental Crust and Its Mineral Deposits, pp. 421–440 Geological Association of Canada Special Paper 20.

Williams, P.F., Price, G.P., 1990. Origin of kinkbands and shear-band cleavage in shear zones: an experimental study. Journal of Structural Geology 12, 145–164.

Yardley, B.W.D., 1989. An Introduction to Metamorphic Petrology. Longman Earth Science, London.

Zen, E-an, 1989. Tectonostratigraphic terranes in the Northern Appalachians: their distribution, origin, and age; evidence for their existence. Fieldtrip Guidebook T359, 28th International Geological Congress, American Geophysical Union, Washington, DC, 66pp.

Zhang, Y., Jessell, M.W., Hobbs, B.E., 1996. Experimental and numerical studies of the accommodation of strain incompatibility on the grain scale. Journal of Structural Geology 18, 451–460.

Zhu, H., Ebel, J.E., 1994. Tomographic inversion for the seismic velocity structure beneath northern New England using seismic refraction data. Journal of Geophysical Research 99, 15331–15357.